REPORT DOCUMENTATION PAGE

Form Approved OMB NO. 0704-0188

1. AGENCY USE ONLY (Leave Blank)	2. REPORT DATE:	3. REPORT TYPE AND DATES COVERED
		Final Report 1-Aug-2002 - 31-Dec-2006

4. TITLE AND SUBTITLE

Characterization and Detection of Delamination in Smart Composite Structures

5. FUNDING NUMBERS

DAAD19-02-1-0355

6. AUTHORS

Hsin-Piao Chen, Aditi Chattopadhyay

8. PERFORMING ORGANIZATION REPORT NUMBER

7. PERFORMING ORGANIZATION NAMES AND ADDRESSES

California State University - Long Beach
6300 State University Dr.

Long Beach, CA 90815 -

9. SPONSORING/MONITORING AGENCY NAME(S) AND ADDRESS(ES)

U.S. Army Research Office
P.O. Box 12211
Research Triangle Park, NC 27709-2211

10. SPONSORING / MONITORING AGENCY REPORT NUMBER

44121-EG-H.3

11. SUPPLEMENTARY NOTES

The views, opinions and/or findings contained in this report are those of the author(s) and should not contrued as an official Department of the Army position, policy or decision, unless so designated by other documentation.

12. DISTRIBUTION AVAILIBILITY STATEMENT

Approved for Public Release; Distribution Unlimited

12b. DISTRIBUTION CODE

13. ABSTRACT (Maximum 200 words)

The abstract is below since many authors do not follow the 200 word limit

14. SUBJECT TERMS

Delamination analysis, delamination detection, smart structures, piezoelectric sensors, neural networks, genetic algorithms, engineering optimization

15. NUMBER OF PAGES

Unknown due to possible attachments

16. PRICE CODE

17. SECURITY CLASSIFICATION OF REPORT	18. SECURITY CLASSIFICATION ON THIS PAGE	19. SECURITY CLASSIFICATION OF ABSTRACT	20. LIMITATION OF ABSTRACT
UNCLASSIFIED	UNCLASSIFIED	UNCLASSIFIED	UL

NSN 7540-01-280-5500

Standard Form 298 (Rev .2-89)
Prescribed by ANSI Std.
239-18 298-102

Report Title

Characterization and Detection of Delamination in Smart Composite Structures

ABSTRACT

A multidisciplinary procedure has been developed for damage diagnosis or interrogation based on the concept of analyzing temporal relations between values of critical variables. Some observable variable of the system is traced through time from a specific initial state. The dynamics of the degradation process can be described by a time-variant mathematical model of this relationship. A novel neural-network-based approach to damage diagnosis and prognosis for nonlinear dynamic systems has been developed. High quality response surface approximations are developed to the progressive damage model. A neural network is trained to model the multi-dimensional response surface that relates the dependent variables to the independent variables. The main advantage of neural networks is that much more complex nonlinear relationships can be modelled, potentially incorporating high order interactions between predictive variables. A distinct feature of the proposed technique for constructing the response surface approximations is that it permits explicit treatment of the dynamics of the process under observation - in this case, structural damage that evolves in time. Assessing and quantifying existing damage may be treated as a static problem and its solution can be summarized by a mapping from parametric descriptions of damage attributes and measured structural response data.

List of papers submitted or published that acknowledge ARO support during this reporting period. List the papers, including journal references, in the following categories:

(a) Papers published in peer-reviewed journals (N/A for none)

Deenadayalu, C. A., Chattopadhyay, A. and Chen, H. P., "Characterization and Detection of Delamination in Composite Laminates Using Artificial Neural Networks," Structural Health Monitoring Journal, Article in press.

Number of Papers published in peer-reviewed journals: 1.00

(b) Papers published in non-peer-reviewed journals or in conference proceedings (N/A for none)

Number of Papers published in non peer-reviewed journals: 0.00

(c) Presentations

Number of Presentations: 0.00

Non Peer-Reviewed Conference Proceeding publications (other than abstracts):

Number of Non Peer-Reviewed Conference Proceeding publications (other than abstracts): 0

Peer-Reviewed Conference Proceeding publications (other than abstracts):

Deenadayalu, C. A., Chattopadhyay, A. and Goldberg, R. K, "General Formulation for Basic Mechanical State Equations of Fatigue-Damage Process in Laminate Composites," To be presented at AIAA/ASME/ASCE/AHS/ASC 48th Structures, Structural Dynamics and Materials Conference, AIAA, Honolulu, HI, 2007.

Deenadayalu, C. A., Chattopadhyay, A. and Zhou, X., "Application of Artificial Neural Networks to the Simulation of Progressive Damage in Composite Laminates," AIAA/ASME/ASCE/AHS/ASC 47th Structures, Structural Dynamics and Materials Conference, AIAA, Newport, RI, 2006.

Deenadayalu, C. A., Chattopadhyay, A. and Zhou, X., "Constitutive Modeling of Progressive Damage in Composite Laminates," AIAA/ASME/ASCE/AHS/ASC 46th Structures, Structural Dynamics and Materials Conference, AIAA, Austin, TX, 2005.

Le, H., Chen, H. P. and Chattopadhyay, A., "Multiple and Generalized Delamination Detections Using Neural Network Technique and Genetic Algorithm," Proceedings of the46th AIAA/ASME/ASCE/AHS/ASC Structures, Structural Dynamics and Materials Conference, 2005.

Chen, H. P. and Kim, J., "A Combined Technique of Genetic Algorithms and Neural Networks for Delamination Detection in Composite Laminates," The Fifth Canadian International Composites Conference, CANCOM 2005, Vancouver, Canada, 2005.

Deenadayalu, C. A., Chattopadhyay, A. and Chen, H. P., "Characterization and Detection of Delamination in Composite Laminates Using Artificial Neural Networks," Presented at AIAA MDO Conference, Albany, NY, 2004.

Chen, H. P., Le, H., Kim, J. and Chattopadhyay, A. "Delamination Detection Problems using a Combined Genetic Algorithm and Neural Network Technique," Proceedings of the 10th AIAA/ISSMO Multidisciplinary Analysis and Optimization Conference, Albany, New York, 2004.

Number of Peer-Reviewed Conference Proceeding publications (other than abstracts): 7

(d) Manuscripts

Number of Manuscripts: 0.00

Number of Inventions:

Graduate Students

NAME	PERCENT_SUPPORTED	
Hieu Le	0.50	No
Jin Kim	0.50	No
Chaitanya Deenadayalu	0.50	No
Sorin Munteanu	0.25	No
Tran Phuong	0.25	No
FTE Equivalent:	**2.00**	
Total Number:	**5**	

Names of Post Doctorates

NAME	PERCENT_SUPPORTED
FTE Equivalent:	
Total Number:	

Names of Faculty Supported

NAME	PERCENT_SUPPORTED	National Academy Member
Hsin-Piao Chen	0.10	No
Aditi Chattopadhyay	0.10	No
FTE Equivalent:	**0.20**	
Total Number:	**2**	

Names of Under Graduate students supported

NAME	PERCENT_SUPPORTED
FTE Equivalent:	
Total Number:	

Names of Personnel receiving masters degrees

NAME	
Jin Kim	No
Total Number:	**1**

Names of personnel receiving PHDs

NAME	
Hieu Le	No
Chaitanya Deenadayalu	No
Total Number:	**2**

Names of other research staff

NAME	PERCENT_SUPPORTED
FTE Equivalent:	
Total Number:	

Sub Contractors (DD882)

Inventions (DD882)

FOREWORD

A traditional approach to fault diagnosis is based on “hardware (or physical/parallel) redundancy” methods which use multiple lanes of sensors, actuators, computers and software to measure and/or control a particular variable. Typically, a voting scheme is applied to the hardware redundant system to decide if and when a fault has occurred and its likely location amongst redundant system components. The use of multiple redundancies in this way is common, for example with digital fly-by-wire flight control systems e.g. the AIRBUS 320 and its derivatives and in other applications as in nuclear reactors. In general, one needs many more sensors and also non-robust sensors in hardware redundancy methods. This may become expensive and more sensitive to sensor-based faults. In contrast, model-based fault detection methods need only some few and possibly robust sensors. Model-based fault detection can provide direct insight into dynamic properties such as the transient response. A fault usually causes changes in several output variables with different signs and dynamics. The model-based fault detection takes into account all these entailed changes, provides a data reduction and determines theoretically the state variable which has been changed directly by the fault. Hence, it can be expected that a significant change in the state variable can be extracted and that the fault detection selectivity is improved.

Compressing computational time to reasonable limits remains a challenge facing both damage interrogation and prognostic modeling. Another key challenge to field deployment of a robust structural health monitoring system is data normalization. System response data is usually measured under varying operational and environmental conditions and without appropriate data normalization procedures changes in the measured response caused by operational and environmental conditions may be mistaken for changes caused by the damage process. These challenges are addressed through a multi-disciplinary approach that incorporates elements from engineering mechanics, mathematical and computational analysis, probability, and computer science.

TABLE OF CONTENTS

LIST OF TABLES

LIST OF FIGURES

PROBLEM STATEMENT AND APPROACH

The primary objective is to develop a model-based diagnostic and prognostic framework for system-level health management. A strategy modeled on the following three-stage approach has been adopted in this work:

1. Quantifying the degree of existing damage.
2. Constitutive modeling of progressive damage.
3. Diagnosing the response of the structure to evaluate the progression of damage over time and develop a prognosis system given knowledge of the damage history.

Quantifying the degree of existing damage

Fault detection is formulated as an optimization problem; it is essentially an inverse multi-modal problem, usually a large number of local optima exist and the traditional gradient-based techniques may result in a trapped local optimum. A stochastic global search method based on the genetic algorithm is adopted to search the optimal solution. An improved laminate theory incorporating a layerwise deformation field is used to model material behavior. An artificial neural network is trained to simulate results from the finite element analysis. The artificial neural network is effectively doing function approximation which is used to associate parameterized descriptions of a given set of damage patterns with their corresponding signatures.

Constitutive modeling of progressive damage

Progressive damage analysis of laminated composites is performed using a micromechanical model. A state variable constitutive formulation for characterizing the nonlinear, strain rate dependent deformation of polymeric materials has been modified in order to accurately account for the effects of damage on their mechanical behavior. The revised polymer constitutive equations have been incorporated into a classical solid mechanics based micromechanics model to predict damage and the consistent reduction of effective composite properties during the various phases of its evolution in time. A finite element program based on a refined layerwise theory is used in the laminate analysis. A macro-micro approach is used to relate the lamina stresses predicted by the global laminate analysis to the micromechanical stresses in each constituent of the composite.

Diagnosis and prognosis

The approach adopted emphasizes damage diagnostics as a prelude to developing reliable damage prognosis solutions. Damage diagnosis or interrogation is treated as a two-step process. First, some observable variable of the system is traced through time from a specific initial state. It is crucial that changes in this variable reflect changes in the damage distribution in the structure. The previously discussed macro-micro finite element analysis program is used to generate sample data for the inverse mapping between structural degradation and the transient response under a given load. The dynamics of the degradation process can then be approximated with a nonlinear autoregressive system. Static mappers have long-term memory, since the information utilized during system training is converted into weight values using the learning rules. They contain a repository of past information that is associated with memory. However,

they are unable to differentiate time relationships, because the information collected through time is collapsed in the weight values. In temporal problems, such as the simulation of progressive damage, the measurements from the world are no longer an independent set of input samples, but functions of time. In temporal phenomena, time imposes a structure in the input space, in other words, the sequence in which the points are visited is important. Time is represented implicitly by its effects on processing rather than explicitly (as in a spatial representation). This involves the use of internal network feedbacks or recurrent links in order to provide networks with a dynamic memory.

SUMMARY OF IMPORTANT RESULTS

Quantifying the degree of existing damage

In this section a comparison is made between the developed model and known solutions to problems. A six-ply orthotropic laminate with $[90/0/90]_{2s}$ stacking sequence and dimensions 6 x 20 x 0.0127 cm was used. Cantilever boundary conditions are used. The orthotropic material properties used were:

$$E_{11} = 134.4\text{GPa} \quad E_{22} = 10.34\text{GPa} \quad G_{12} = 5.0\text{GPa}$$
$$\nu_{12} = 0.33 \qquad \rho = 1477\text{kgm}^{-3} \tag{1}$$

Only rectangular delaminations were considered. Two different types of delaminations – through-the-width and seeded, are considered in the current study. The direct problem is computed on a finite element grid consisting of 147 nodes and 120 quadrilateral plate elements. Due to the symmetry of the lay-up with respect to the laminate mid-plane, only damage occurring in the upper half of the laminate is considered. The position of the damage zone is varied along the length, width, and depth of the plate; from the fixed end to the free end along the length, edge to edge along the width, and mid-plane to slightly below the top surface along the depth. Finite element analysis is used to estimate the damage indices evolving from all the different damage patterns. The training data consists of parameterized descriptions of individual damage patterns with their corresponding damage index signatures.

The data prepared were divided into training, cross validation and testing sets. The training set is used to adjust the network weights *i.e.*, to teach the network. When the trained model is utilized for new inputs never encountered before, it will produce for each input a response based on the parameters obtained during training. If the new data comes from the same set, that is, the training set, the response should resemble the value of the desired response for that particular input value, that is, the model should have the ability to extrapolate responses for new/unseen data. This is an important feature, since in general it is desirable that the performance obtained in the training set also applies or generalizes to the new/unseen data when the model is deployed. The test set used to verify the model performance consists of a combination of data from the training set and new/unseen data not used for training but for which the desired response (damage index distribution) is still known.

Traditional knowledge from data modeling and recent developments in learning theory (Vapnik, 1995) clearly indicate that after a critical point a network trained with backpropagation will continue to do better in the training set, but the test set performance will begin to deteriorate - the learning algorithm over-fits the training data. This phenomenon is called overtraining. The current framework circumvents this problem by stopping the training at the point of maximum generalization (given the present data and

the architecture of the network). This is called early stopping, or stopping with cross-validation. The cross-validation set is normally taken as 10 percent of the total training samples. At regular intervals (*i.e.,* 5 to 10 iterations), the network performance with the present weights is tested against the cross-validation set. Training should be stopped when the error in the cross-validation set starts to increase. This point is the point of maximum generalization or the point of the smallest error in the cross-validation set.

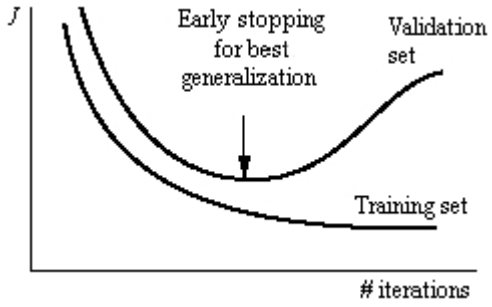

Figure 1 Generalization

The investigation was made with a three-layer network; the structure of the network is expressed as $n_{\mathrm{p}} - S^1 - S^2 - n_{\mathrm{m}}$, where n_{p} is the dimension of the input space, S^1, S^2 are the number of PEs in the first and second hidden layers, and n_{m} is the higher (finite or even infinite) dimensional "feature space" in which the patterns become separable, in this case, the number of points in the damage index distribution used to detect the delamination. The choice of number of units for the input and output layers is a function of the representation; the choice for the hidden layers is determined heuristically – 70 and 2100 PEs were found to be adequate for the first and second hidden layers, respectively.

As a first step, the network was trained to simulate the response to through-the-width delamination; it was trained with 294 data sets, which included both descriptions of through-the-width delaminations and the corresponding damage index distributions. The network output fitted the simulation results with a mean square error of 0.00001. The multi-layered network was found to converge in a relatively small number of iterations. However, each iteration took considerable time because of the relatively large number (70 and 2100, in this particular case) of hidden PEs required for the training. The resulting trained network was, however, found to fit the simulations quite well, with a relative mean error of 0.5%, which is acceptable for the current problem.

The genetic algorithm (GA) was customized for detecting through-the-width delaminations. This GA consists of a selection operator, two genetic operators (crossover or recombination and mutation) with associated probabilities, and a termination criterion. In addition, an elitist strategy (De Jong, 1975), in which the best individual found survives and is selected by the next generation, was adopted in this tailored version. In the present numerical simulations, the selection technique employed a "tournament selection" (Goldberg and Deb, 1991) mechanism, in which a set of three individuals is picked at random and the best individual in this set is then selected by the mating group. The basic operator for producing new individuals in the GA is that of crossover with a probability of 0.6. Uniform mutation, with a probability of 0.4, is applied. Typically, a

population was composed of 80 individuals and the GA was set to terminate after 1000 generations, a number that was determined by judicious use of heuristic cues. However, the algorithm is terminated early if it converges to a satisfactory solution before 1000 generations. Seventeen delamination patterns were considered and the results are listed in Table 1. The delamination patterns chosen to verify the neural network performance in this case represent the smallest possible through-the-width damage that can be modeled in this particular FE mesh (20x6) chosen to model the cantilever plate. Their damage index distributions were predicted using a well-trained neural network. The actual delamination pattern corresponding to a given damage index distribution and the GA-predicted delamination pattern are listed in Table 1.

The problem of detecting seeded delaminations is made complicated by the fact that a total of five parameters (shown in Fig 2) are required to describe the delamination, as opposed to three in the case of through-the-width delaminations. The network was trained with 98 data sets for each value of z_d. Since there are three permissible values of z_d (0, 1, and 2), there were totally 294 training data sets generated using finite element analysis.

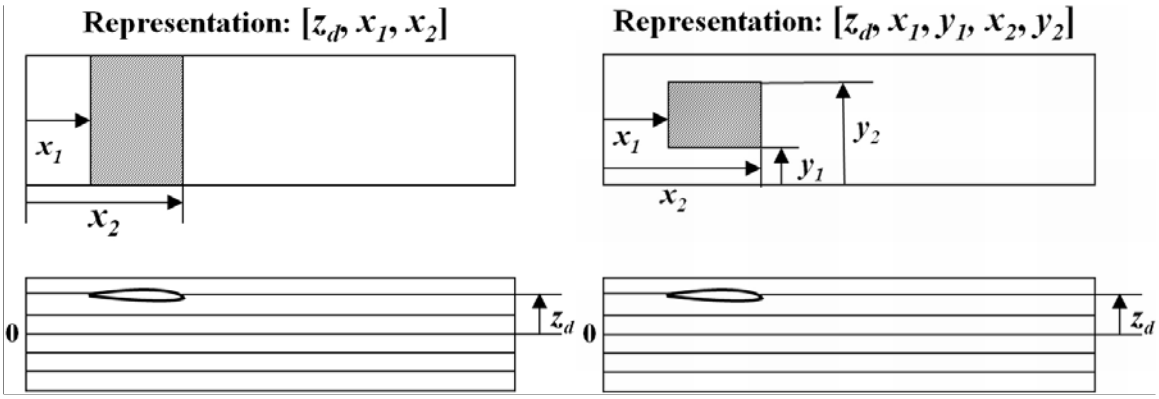

Figure 2 Input-space representations of through-the-width and seeded damage, respectively.

Two different approaches were experimented with in the construction of the neural network model. The first approach was similar to that used for though-the-width delaminations in which a single network was constructed. However, the input vector has five parameters describing the delamination. The validation error of this model was much larger than 0.5%, which was the relative mean error of the model for the through-the-width delamination problem. It was found that a single network model working in conjunction with GA was not able to locate and describe seeded delaminations accurately. It is noted that although both models employed an identical number of training sets (294), the accuracy of the model simulating seeded delaminations is much lower since the problem is more complicated with a higher number of descriptive parameters involved.

Table 1.
Detecting through-the-width delaminations with current technique.

Case	Actual delamination pattern $[z_d, x_1, x_2]_{actual}$	Predicted delamination pattern $[z_d, x_1, x_2]_{predicted}$
1	[0, 5.0, 7.0]	[0, 4.99, 7.02]
2	[0, 8.0, 10.0]	[0, 8.01, 9.98]
3	[0, 11.0, 13.0]	[0, 10.98, 13.01]
4	[0, 14.0, 16.0]	[0, 14.03, 16.04]
5	[0, 17.0, 19.0]	[0, 16.97, 18.98]
6	[1, 2.0, 4.0]	[1, 2.02, 3.98]
7	[1, 5.0, 7.0]	[1, 5.01, 6.99]
8	[1, 8.0, 10.0]	[1, 7.99, 10.02]
9	[1, 11.0, 13.0]	[1, 10.97, 12.98]
10	[1, 14.0, 16.0]	[1, 14.01, 15.98]
11	[1, 17.0, 19.0]	[1, 16.95, 19.04]
12	[2, 2.0, 4.0]	[2, 1.99, 4.01]
13	[2, 5.0, 7.0]	[2, 4.97, 6.97]
14	[2, 8.0, 10.0]	[2, 8.03, 9.98]
15	[2, 11.0, 13.0]	[2, 10.95, 12.98]
16	[2, 14.0, 16.0]	[2, 14.05, 16.04]
17	[2, 17.0, 19.0]	[2, 16.89, 19.05]

Since the first approach was not successful, an alternate approach was developed which improved the accuracy of the function approximation. Note that there are only three permissible values (0, 1, and 2) for the first input variable z_d. Therefore, instead of using a single network model, three individual neural network modules were constructed in this approach. A neural network module was constructed, using 98 training data sets and 75 cross validation data sets, corresponding to each value of z_d. Therefore, the input vector of each module now consisted of only four real variables, $[x_1, y_1, x_2, y_2]$. The validation errors of these three modules are much lower than that of the single neural network model.

As in the previous case, a genetic algorithm was tailored for detecting seeded delaminations. This is an elitist GA employing (1) the tournament selection mechanism, with a size of three, (2) the one-point crossover operator with a probability of 0.6 and (3) the uniform mutation operator with a probability of 0.4. The population was composed of 80 individuals. The GA iterates around the generational loop until a pre-specified number of generations – 1000, in this particular case, and then terminates.

The developed framework has been used to detect delamination in composite plates with delaminations located at various ply interfaces. Studies have been conducted for twelve different seeded delamination patterns. The length and the width of the delaminations in the test set are limited to 2 cm and 4 cm, respectively (representing 6.67% of the surface area of the plate). The results are listed in Table 2. The actual delamination pattern corresponding to a given damage index distribution and the GA-predicted delamination pattern are listed. It is observed that all delamination patterns have been identified successfully and precisely using this modular approach.

Table 2
Detecting seeded delaminations with current technique.

Case	Actual delamination pattern $[z_d, x_1, y_1, x_2, y_2]_{actual}$	Predicted delamination pattern $[z_d, x_1, y_1, x_2, y_2]_{predicted}$
1	[0, 2.00, 1.00, 4.00, 5.00]	[0, 1.99, 1.01, 4.01, 4.97]
2	[0, 7.00, 1.00, 9.00, 5.00]	[0, 7.02, 1.01, 8.98, 5.03]
3	[0, 12.00, 1.00, 14.00, 5.00]	[0, 11.98, 0.98, 13.98, 4.95]
4	[0, 17.00, 1.00, 19.00, 5.00]	[0, 16.96, 0.97, 19.02, 4.93]
5	[1, 2.00, 1.00, 4.00, 5.00]	[1, 2.01, 0.99, 4.02, 4.99]
6	[1, 7.00, 1.00, 9.00, 5.00]	[1, 7.03, 1.01, 8.98, 5.02]
7	[1, 12.00, 1.00, 14.00, 5.00]	[1, 11.97, 1.02, 14.01, 4.97]
8	[1, 17.00, 1.00, 19.00, 5.00]	[1, 17.05, 0.97, 19.03, 4.93]
9	[2, 2.00, 1.00, 4.00, 5.00]	[2, 2.02, 0.97, 4.01, 4.98]
10	[2, 7.00, 1.00, 9.00, 5.00]	[2, 6.98, 1.01, 9.01, 5.02]
11	[2, 12.00, 1.00, 14.00, 5.00]	[2, 12.04, 1.01, 13.97, 5.02]
12	[2, 17.00, 1.00, 19.00, 5.00]	[2, 16.89, 0.90, 19.05, 4.92]

A similar approach has been improvised for detecting multiple seeded delaminations. The representation is a mixed type data structure containing 10 variables (shown in Fig 3). Three individual neural network modules were constructed in this approach for each delamination. A neural network module was constructed corresponding to each value of z_d for each delamination. As before, the input vector of each module now consisted of only four real variables, $\left[x_d, y_d, a_x, a_y\right]$. The validation error for each of these modules was less that 0.3% which is acceptable.

Numerical studies have been conducted for nine different delamination configurations and the results are presented in Table 3. Each of the nine configurations in the test set comprises two discrete, but identical (in size) seeded delaminations, both located at the same through-the-thickness location. The actual delamination pattern corresponding to a given damage index distribution and the GA-predicted description are listed. It is observed that all delamination patterns have been identified successfully and described accurately using this modular approach.

The same modular approach may be employed to detect and describe overlapping delaminations. The representation is a mixed type data structure containing 10 variables (shown in Fig 3). A neural network module was constructed, from a training set where the total delamination size varies from 15 to 40% and the delaminations may overlap each other by anywhere between 15 to 75%, corresponding to each value of z_d for each delamination. Again, the input vector of each module now consisted of only four real variables, $\left[x_d, y_d, a_x, a_y\right]$. The validation error for each of these modules was less than 0.3% which is acceptable. Studies have been conducted for nine different delamination configurations and the actual delamination pattern corresponding to a given damage index distribution and the GA-predicted delamination pattern are reported in Table 4. Each of the nine configurations in the test set comprises two overlapping, but identical (in size) seeded delaminations.

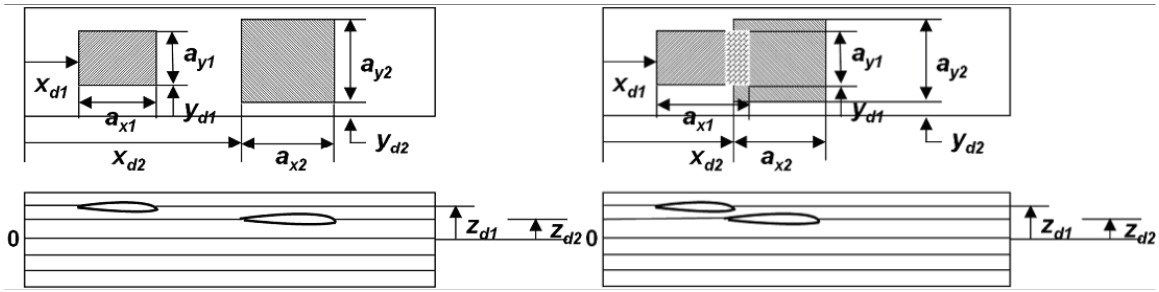

Figure 3 Input-space representations of discrete seeded multiple and seeded overlapping damage, respectively.

Table 3
Detecting discrete multiple seeded delaminations with current technique.

Case	Actual delamination pattern $\left[z_d, x_d, y_d, a_x, a_y\right]_{actual}$	Predicted delamination pattern $\left[z_d, x_d, y_d, a_x, a_y\right]_{predicted}$
1	[0, 12.00, 1.00, 2.00, 4.00] $_1$	[0, 11.97, 0.98, 1.97, 3.96] $_1$
	[0, 15.00, 1.00, 2.00, 4.00] $_2$	[0, 14.96, 1.03, 1.96, 4.04] $_2$
2	[0, 14.00, 1.00, 2.00, 4.00] $_1$	[0, 14.03, 0.96, 2.02, 4.02] $_1$
	[0, 17.00, 1.00, 2.00, 4.00] $_2$	[0, 17.05, 0.96, 2.02, 3.98] $_2$
3	[1, 7.00, 1.00, 2.00, 4.00] $_1$	[1, 7.02, 0.98, 1.97, 4.02] $_1$
	[1, 10.00, 1.00, 2.00, 4.00] $_2$	[1, 10.02, 0.98, 1.96, 3.97] $_2$
4	[1, 12.00, 1.00, 2.00, 4.00] $_1$	[1, 11.97, 1.03, 2.01, 3.97] $_1$
	[1, 15.00, 1.00, 2.00, 4.00] $_2$	[1, 14.96, 0.97, 1.98, 4.03] $_2$
5	[1, 14.00, 1.00, 2.00, 4.00] $_1$	[1, 13.95, 1.03, 1.96, 3.97] $_1$
	[1, 17.00, 1.00, 2.00, 4.00] $_2$	[1, 16.96, 1.01, 2.03, 4.03] $_2$
6	[2, 2.00, 1.00, 2.00, 4.00]$_1$	[2, 2.01, 0.97, 2.01, 3.97] $_1$
	[2, 5.00, 1.00, 2.00, 4.00] $_2$	[2, 5.02, 1.01, 2.01, 4.00] $_2$
7	[2, 7.00, 1.00, 2.00, 4.00] $_1$	[2, 6.98, 0.98, 2.01, 4.03] $_1$
	[2, 10.00, 1.00, 2.00, 4.00] $_2$	[2, 9.98, 1.02, 1.98, 3.98] $_2$
8	[2, 12.00, 1.00, 2.00, 4.00] $_1$	[2, 12.02, 1.01, 1.96, 4.03] $_1$
	[2, 15.00, 1.00, 2.00, 4.00] $_2$	[2, 15.04, 1.02, 2.00, 4.03] $_2$
9	[2, 14.00, 1.00, 2.00, 4.00] $_1$	[2, 13.92, 0.96, 1.95, 3.96] $_1$
	[2, 17.00, 1.00, 2.00, 4.00] $_2$	[2, 16.95, 1.01, 1.95, 3.96] $_2$

The damage index is evaluated at each layer-integration point within each lamina, within each element. Thus, training a neural network to associate parameterized descriptions of a given set of damage patterns with their corresponding damage index signatures in the discrete form is computationally expensive and the resulting trained network requires extensive amounts of data to be of any use as a simulation tool. A transformation is necessary to cast the data into a form that will allow the network to learn, recognize, and reproduce the training data. Such a transformation can be developed using the Gaussian kernel.

$$G(\delta) = g_1 \exp\left(-\left(\frac{\delta - g_2}{g_3}\right)^2\right) \tag{2}$$

Table 4
Detecting overlapping seeded delaminations with current technique.

Case	Actual delamination pattern $\left[z_d, x_d, y_d, a_x, a_y\right]_{actual}$	Predicted delamination pattern $\left[z_d, x_d, y_d, a_x, a_y\right]_{predicted}$
1	[0, 12.00, 1.00, 2.00, 4.00] $_1$	[0, 11.97, 0.98, 1.97, 3.98] $_1$
	[1, 13.00, 1.00, 2.00, 4.00] $_2$	[1, 13.01, 1.00, 1.98, 3.97] $_2$
2	[0, 14.00, 1.00, 2.00, 4.00] $_1$	[0, 14.02, 0.97, 2.02, 4.02] $_1$
	[1, 15.00, 1.00, 2.00, 4.00] $_2$	[1, 14.98, 1.01, 2.00, 3.97] $_2$
3	[0, 16.00, 1.00, 2.00, 4.00] $_1$	[0, 16.04, 1.03, 1.98, 4.02] $_1$
	[1, 17.00, 1.00, 2.00, 4.00] $_2$	[1, 17.02, 0.99, 1.99, 4.00] $_2$
4	[2, 2.00, 1.00, 2.00, 4.00] $_1$	[2, 2.01, 1.01, 1.99, 4.00] $_1$
	[1, 3.00, 1.00, 2.00, 4.00] $_2$	[1, 2.99, 1.01, 2.01, 4.00] $_2$
5	[2, 7.00, 1.00, 2.00, 4.00] $_1$	[2, 6.99, 0.98, 2.02, 3.97] $_1$
	[1, 8.00, 1.00, 2.00, 4.00] $_2$	[1, 8.00, 1.01, 2.01, 3.99] $_2$
6	[2, 12.00, 1.00, 2.00, 4.00] $_1$	[2, 12.02, 1.02, 1.98, 3.98] $_1$
	[1, 13.00, 1.00, 2.00, 4.00] $_2$	[1, 13.01, 1.01, 2.02, 3.98] $_2$
7	[2, 14.00, 1.00, 2.00, 4.00] $_1$	[2, 13.97, 1.02, 1.98, 4.02] $_1$
	[1, 15.00, 1.00, 2.00, 4.00] $_2$	[1, 15.01, 0.99, 2.01, 4.02] $_2$
8	[2, 16.00, 1.00, 2.00, 4.00] $_1$	[2, 15.98, 0.97, 1.98, 4.01] $_1$
	[1, 17.00, 1.00, 2.00, 4.00] $_2$	[1, 16.97, 1.00, 2.01, 4.02] $_2$
9	[2, 7.00, 1.00, 3.00, 4.00] $_1$	[2, 7.01, 1.00, 3.01, 4.01] $_1$
	[1, 9.00, 1.00, 3.00, 4.00] $_2$	[1, 8.99, 0.98, 2.98, 3.98] $_2$

A simple example used in the verification of the approach involves a $[0/90]_{4s}$ carbon/epoxy cantilever plate of dimensions: 5 x 20 x 0.2032 cm. The direct problem was computed on a finite element grid consisting of 126 nodes and 100 quadrilateral plate elements. Due to the symmetry of the lay-up with respect to the laminate mid-plane, only damage occurring in the upper half of the laminate was considered. The position of the damage zone was varied along the length, width, and depth of the plate; from the fixed end to the free end along the length, edge to edge along the width, and mid-plane to slightly below the top surface along the depth. The size of the damage zone was varied from 10 to 20% for through-the-width damage and 4 to 12% for discrete damage. A total of 384 and 3456 distinct patterns were generated with through-the-width and discrete damage conditions, respectively. Finite element analysis was used to estimate the damage indices that arise from all the different damage patterns. The response surface for the damage index (δ) distribution for any given damage pattern can be obtained by computing it for some selected design points in the domain. A Gaussian response surface is fitted to these points by minimizing the squared error between the predicted and the true value at the selected locations. 95% confidence bounds are approximated for each coefficient in the kernel to determine the goodness-of-fit. The response curves for the damage index for two sets of training samples, one each for through-the-width and seeded delaminations are shown in Figs. 4 and 5, respectively. A decrease in computational expense by a factor of a few hundreds (Fig. 6) can be achieved by training the network with the transformed data i.e., the kernel coefficients, with the potential for a large reduction in data requirements of the trained network within an SHM framework

that may include fault diagnosis and on-line control. The training data consists of parameterized descriptions of individual damage patterns and the Gaussian kernel coefficients formally computed for individual responses.

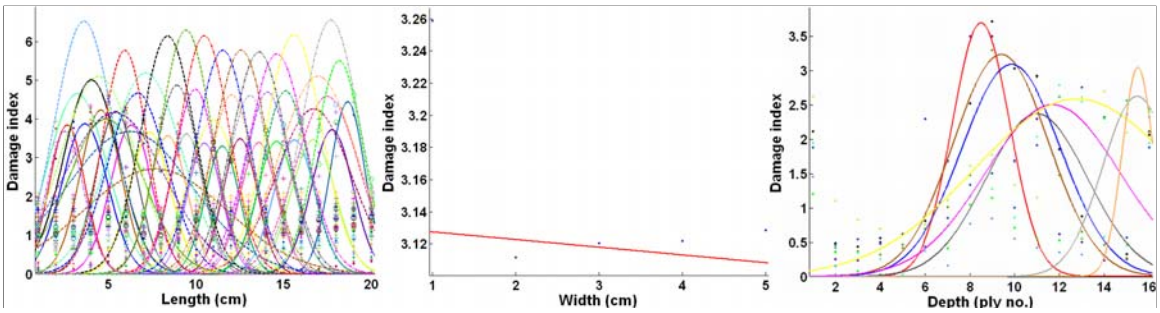

Figure 4 Response curves for damage index distributions, for through-the-width damage patterns, along length, width, and depth of plate, respectively.

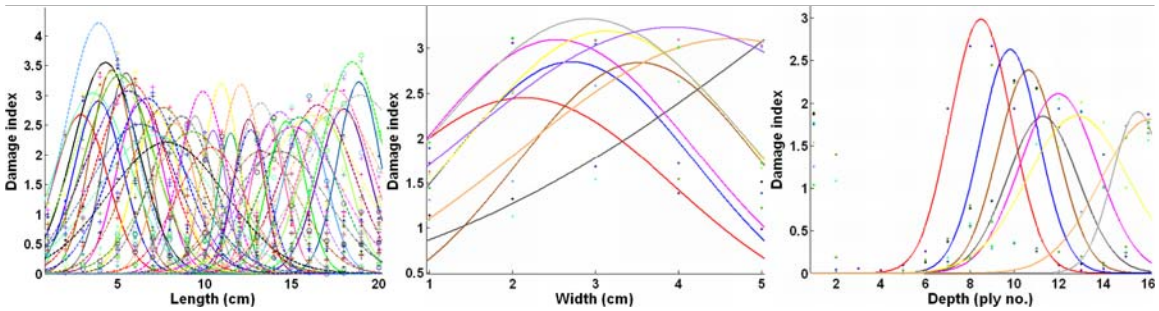

Figure 5 Response curves for damage index distributions, for seeded damage patterns, along length, width, and depth of plate, respectively.

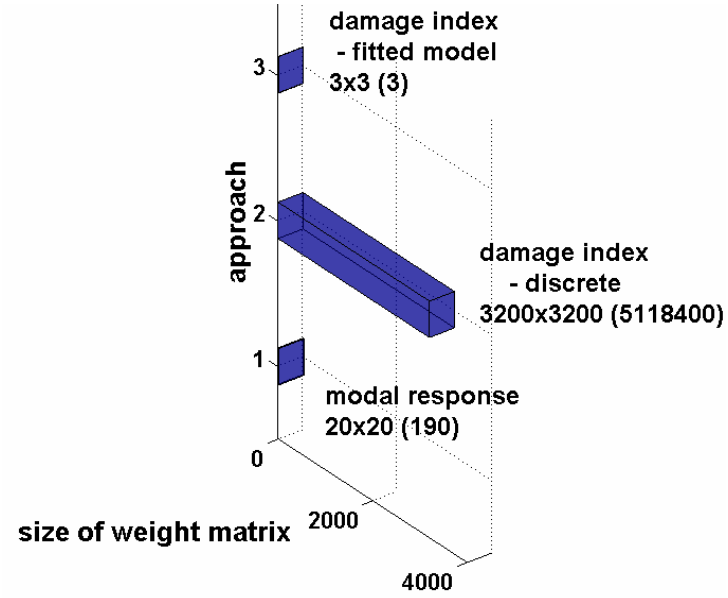

Figure 6 Size of largest weight matrix.

The performance of the trained network is measured by performing a regression analysis between the network response and the corresponding targets. The correlation

coefficient between the outputs and targets is a measure of how well the variation in the output is explained by the targets; if this number is equal to 1, there is perfect correlation between targets and outputs. In the example shown (Fig. 7), the number is very close to 1, which indicates a good fit. The mean values of a relative square error for training data were obtained as 0.5% and 0.05% for through-the-width and seeded damage, respectively. The mean values of a relative error for cross-validation data were obtained as 6.2% and 4.7% for through-the-width and seeded damage, respectively. These values clearly indicate that both networks are capable of generalization.

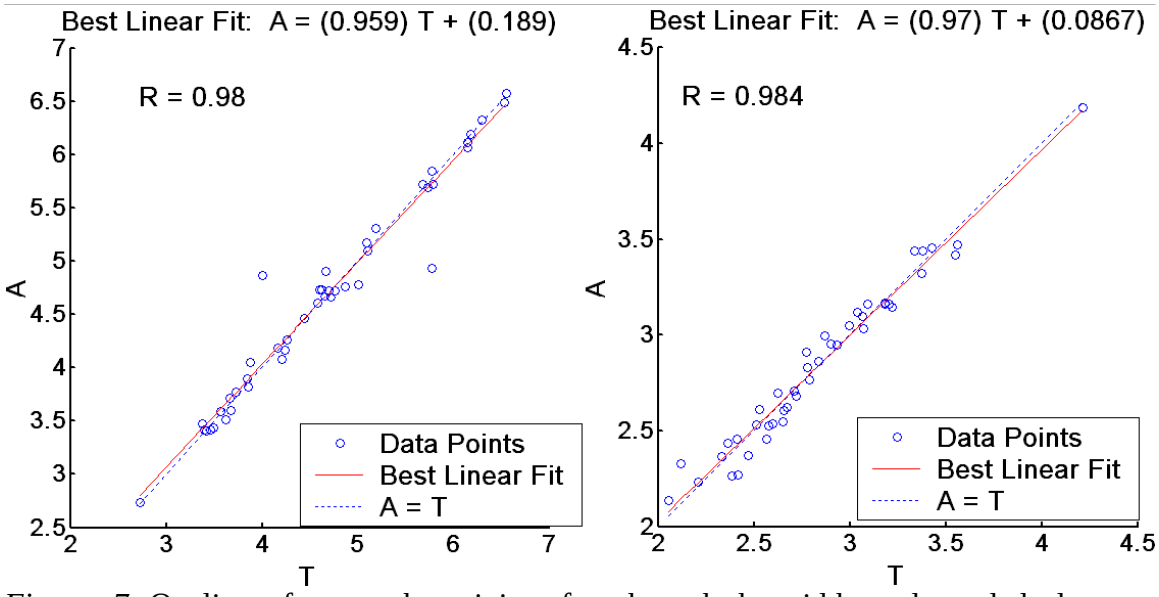

Figure 7 Quality of network training for through-the-width and seeded damage, respectively.

The damage detection problem is again formulated as an optimization problem, posed in the form:

$$\begin{aligned} &Minimize \;\; f(g_i(x), i = 1,2,3) \\ &subject\ to\ l \le x \le u \end{aligned} \tag{3}$$

where the design variable x describes the damage geometry and location. Now, the goal is to minimize the maximum relative absolute error in the Gaussian kernel constants; the objective function is defined as:

$$f = \max_i \left(\left| \frac{g_i^{sim} - g_i^{mea}}{g_i^{mea}} \right| \right) \tag{4}$$

The superscripts $"sim"$ and $"mea"$ denote the simulated and measured values of the kernel constants. Note that, now, the objective function f is a function of the Gaussian kernel constants g_i, which, in turn, are related through the network weights to the design variable x. Six randomly selected examples for each damage condition (through-the-width and discrete) are shown in Table 5. The test set used to verify the model performance consists of a combination of data from the training set and new/unseen data not used for training but for which the desired response (the Gaussian

kernel coefficients) is still known. Plots of the kernel function, actual and simulated, for through-the-width and seeded damage, are shown in Figs. 8 through 13. Note that, in the following figures, X corresponds to the length direction, Y, the width, and Z, the depth of the plate.

Table 5
Through-the-width and seeded delamination detections with trained neural networks.

Case	Through-the-width			Seeded		
	Actual	GA/ANN	Error (%)	Actual	GA/ANN	Error (%)
1	[0 9 11][a]	[0 9 11]	3.2	[4 3 1 6 4][b]	[4 3 1 6 4]	0.7
2	[7 14 18]	[7 14 18]	0.03	[1 13 0 16 4]	[1 13 0 16 4]	1.1
3	[2 10 12]	[2 10 12]	0.4	[2 7 0 10 4]	[2 7 0 10 4]	0.9
4	[4 15 17]	[4 15 17]	0.5	[6 10 0 14 2]	[6 10 0 14 2]	0.9
5	[6 9 12]	[6 9 12]	0.2	[6 4 0 8 2]	[6 4 0 8 2]	0.8
6	[2 16 19]	[2 16 19]	8.9	[6 5 0 8 2]	[6 5 0 8 2]	0.8

[a, b] The representations are explained in Fig. 2.

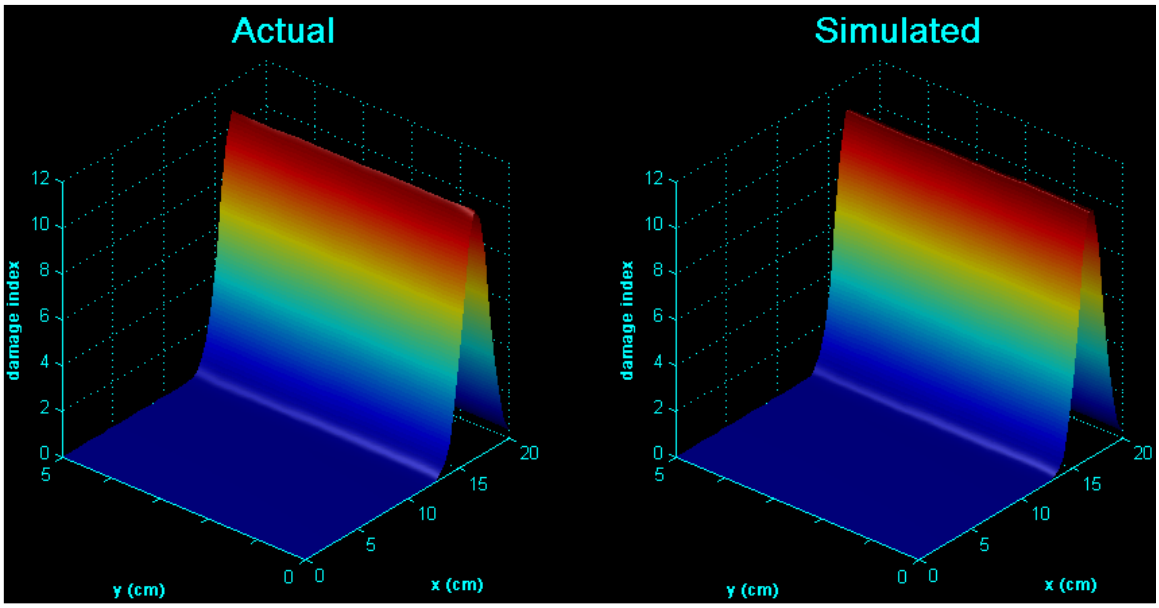

Figure 8 Comparison of kernel functions, actual and as determined by GA/ANN for a through-the-width damage pattern, [4 15 17], in the XY plane.

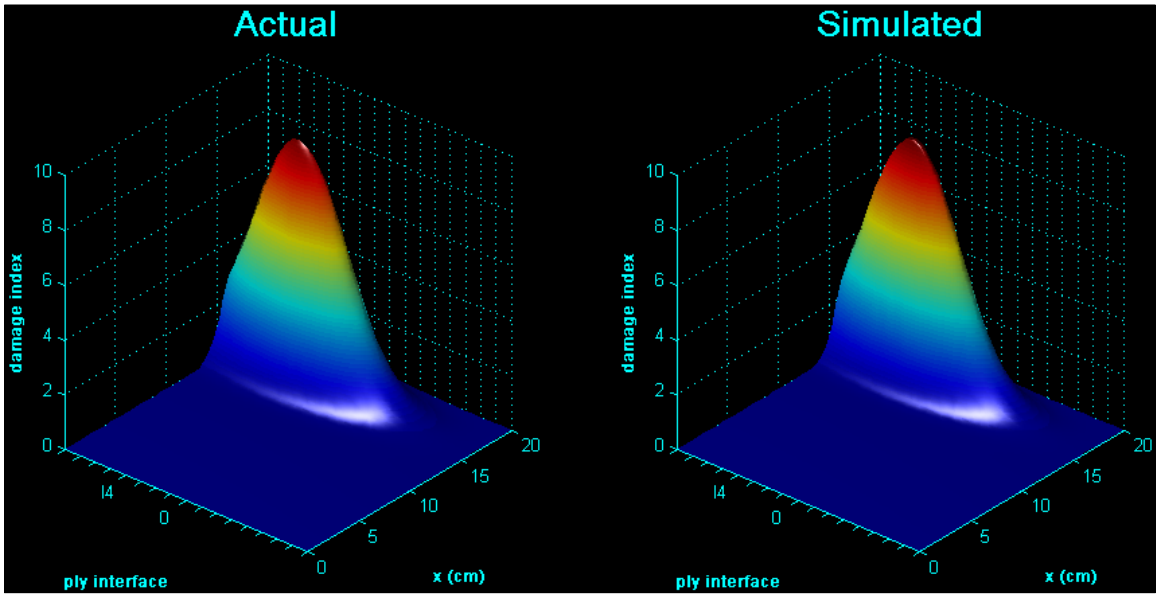

Figure 9 Comparison of kernel functions, actual and as determined by GA/ANN for a through-the-width damage pattern, [4 15 17], in the XZ plane.

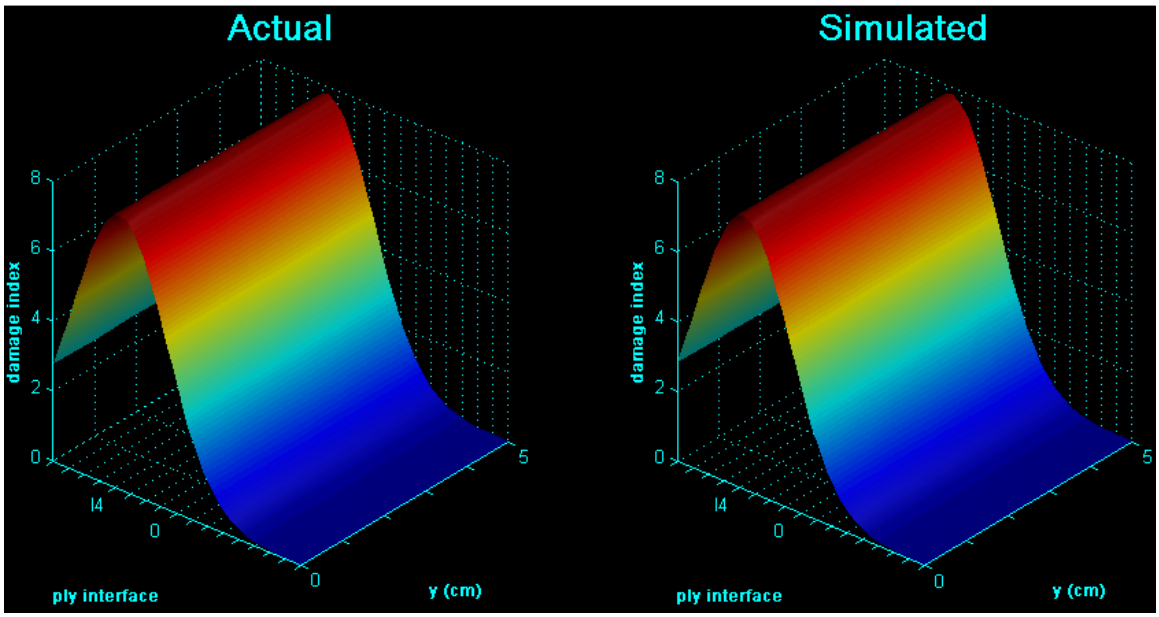

Figure 10 Comparison of kernel functions, actual and as determined by GA/ANN for a through-the-width damage pattern, [4 15 17], in the YZ plane.

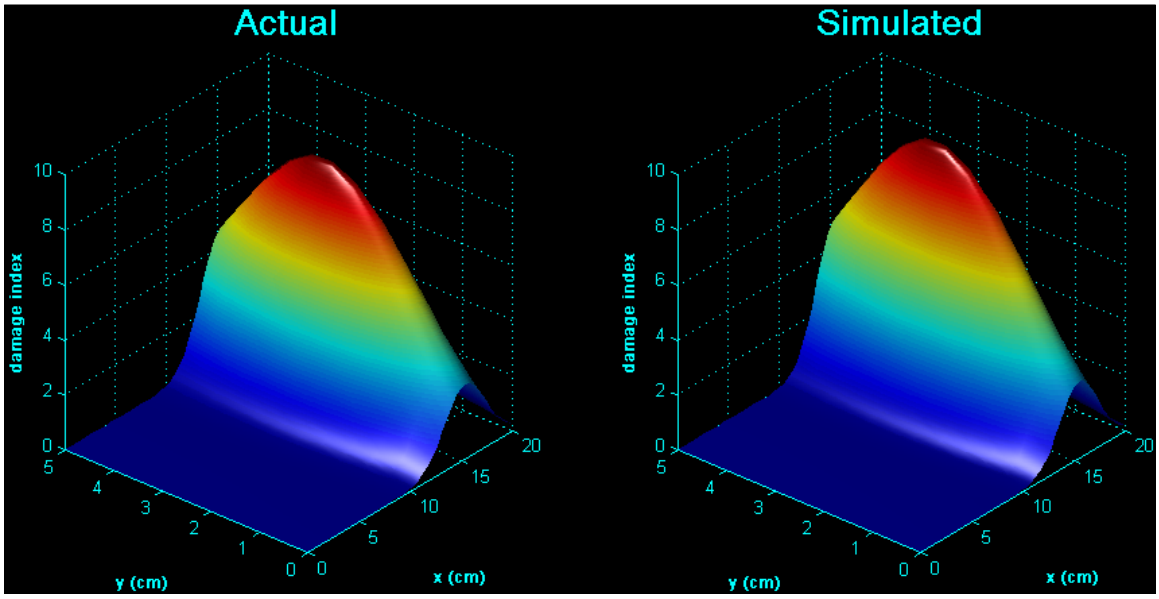

Figure 11 Comparison of kernel functions, actual and as determined by GA/ANN for a seeded damage pattern, [1 13 0 16 4], in the XY plane.

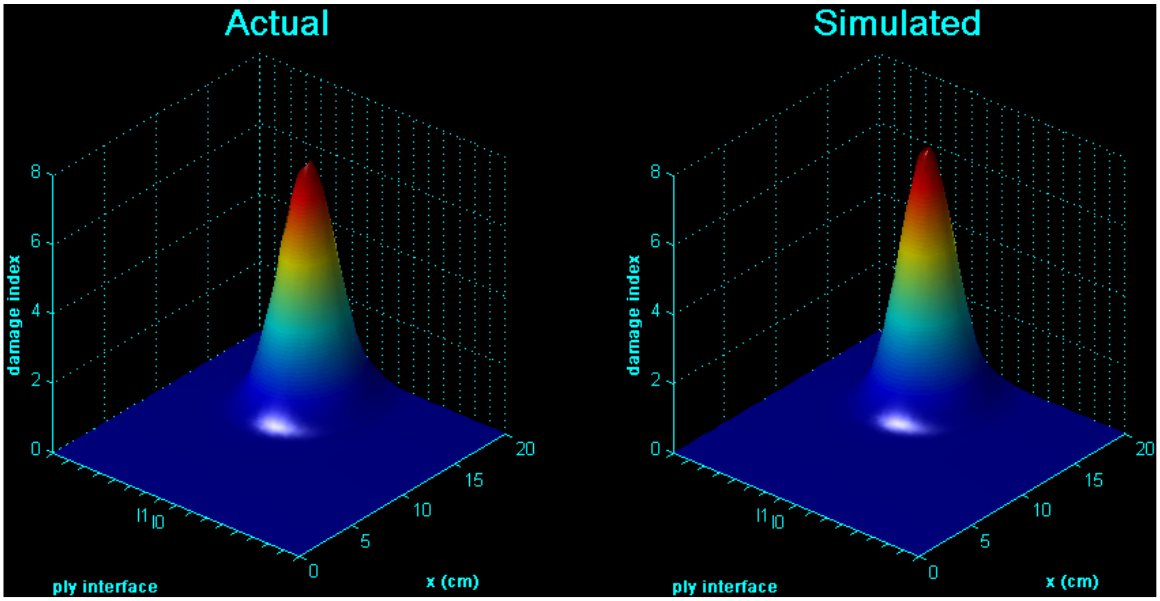

Figure 12 Comparison of kernel functions, actual and as determined by GA/ANN for a seeded damage pattern, [1 13 0 16 4], in the XZ plane.

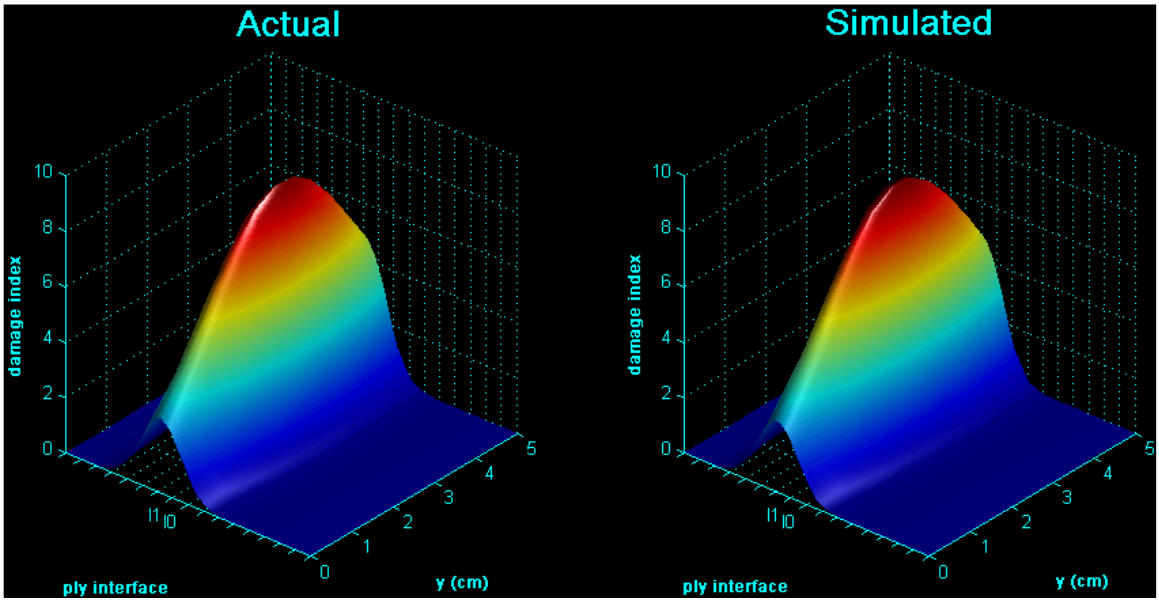

Figure 13 Comparison of kernel functions, actual and as determined by GA/ANN for a seeded damage pattern, [1 13 0 16 4], in the YZ plane.

Constitutive modeling of progressive damage

To study the validity of the developed progressive damage model it is necessary to compare the simulation results with experimental data. The material used in the current study is M30/949 graphite/epoxy. The constituent properties of M30 carbon fibers and 949 epoxy are given in Table 6. Using these values for constituent properties and a fiber volume fraction of 60 percent, effective composite properties are calculated using the micromechanical model.

Table 6
Material properties of the fiber and matrix.

M30 fibers					
E_{11} (GPa)	E_{22} (GPa)	G_{12} (GPa)	G_{23} (GPa)	ν_{12}	ν_{23}
276	13.8	20	5.52	0.25	0.25
949 polymer matrix					
$\dot{\varepsilon}$ (/sec)	E (GPa)	ν	D_0 (/sec)	n	Z_0 (MPa)
9E-5	3.52	0.4	1.00E+06	0.8515	259.496
1.9	3.52	α_0	α_1	q	Z_1 (MPa)
500	6.33	0.1289	0.15215	150.498	1131.371

In the first example problem, a single unidirectional lamina of the fiber-reinforced composite material is subjected to a monotonically increasing, in-plane shear loading ($\sigma_1 = \sigma_2 = 0, \sigma_6 \neq 0$) that produces a state of homogeneous deformation and stress. The

constitutive model is solved incrementally with the applied shear loading imposed in a series of 10 equal load increments and the model predictions are compared with experimental data from Barbero and De Vivo (2001). Comparison of model and experimental shear results are shown in Figure 14.

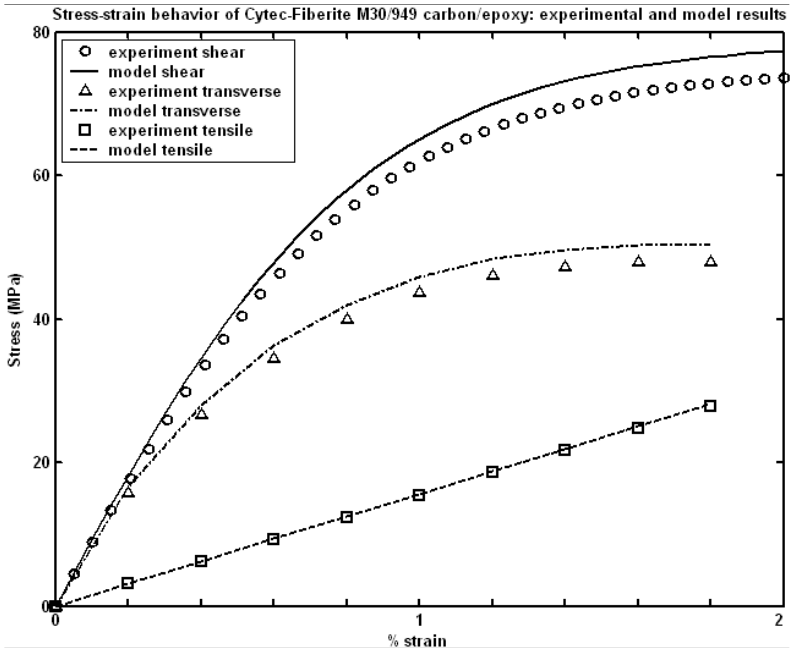

Figure 14 Stress-strain behavior of Cytec-Fiberite M30/949 carbon/epoxy: experimental and model results.

The predicted stress-strain curve in the fiber direction is linear up to failure, as is routinely observed during materials testing. The transverse stress-strain curve shows nonlinearity due to the fact the material is much weaker in the transverse direction than the fiber direction causing matrix cracking in planes perpendicular to the transverse direction. A close examination of the predicted secant stiffness, shown in Figure 15, reveals that damage takes place in all three modes of loading; however, the rate of degradation of the transverse stiffness and the in-plane shear stiffness is orders of magnitude larger than the rate of growth of damage in the fiber direction. The in-plane shear stress-strain curve exhibits a pronounced nonlinearity due to this accelerated damage growth.

The second problem involves a simply-supported, square, symmetric, cross-ply laminate [0/90]s subjected to a uniform pressure. The laminate has a length to thickness ratio of 10. The pressure is applied over a series of 10 uniform load increments, resulting in a maximum load intensity of 19.427 MPa. The constitutive model is solved incrementally and the resulting load deflection response is compared with the solution derived by Robbins Jr. et al (2004). Figure 16 illustrates the nonlinear relationship between the transverse deflection of the plate center and the transverse load intensity caused by the accumulation of distributed microscopic damage. It is observed that the center deflection reaches 10% of its overall thickness without significant nonlinearity due to damage accumulation. However, by the time the center deflection reaches 20% of its overall thickness, a noticeable amount of damage has accumulated and at the peak value

of the pressure, local failure of the matrix is observed at a few points. While the overall load deflection response of the laminate does not exhibit a pronounced nonlinearity, many local points experience appreciable damage accumulation and exhibit severely nonlinear behavior, even complete failure in some cases. The response shown in Figure 16 is a gross behavior produced by the sum of all the material points in the laminate.

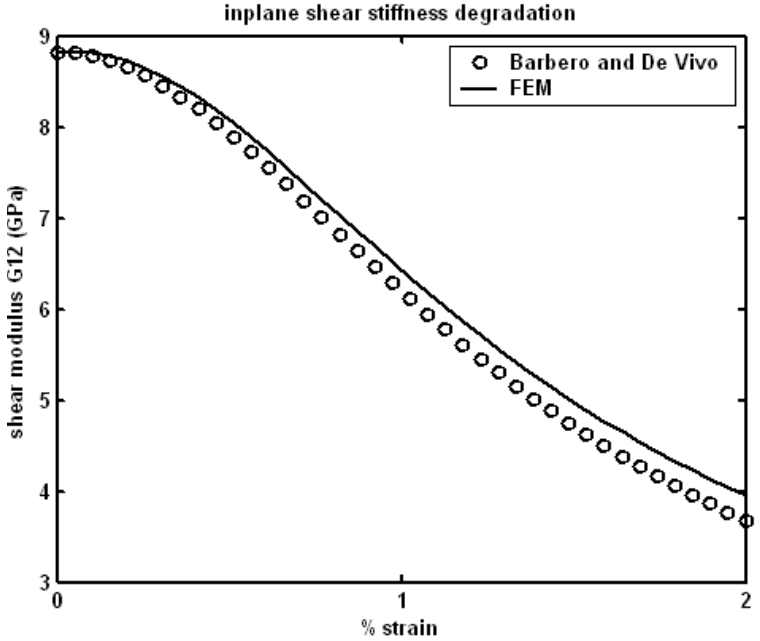

Figure 15 Stiffness degradation of M30/949 carbon/epoxy: experimental and model results.

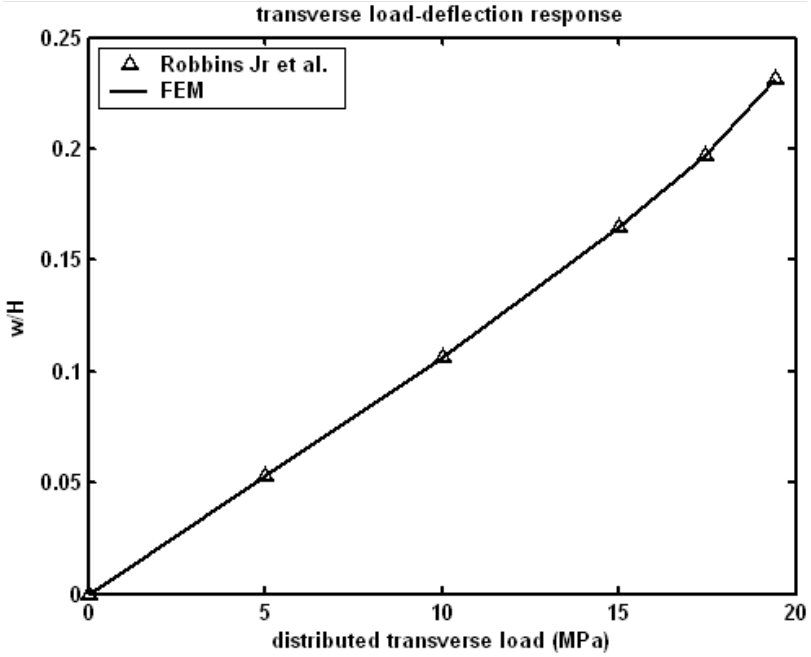

Figure 16 Load-deflection behavior of a simply supported, square, symmetric cross ply laminate subjected to a uniform pressure.

Diagnosis and prognosis

In prediction the goal is to approximate the next sample as a nonlinear combination of past input samples, given by the size of the tap delay line. The desired signal is the input advanced by n_0 samples. The case when $n_0 = 1$ is called single-step prediction. Multi-step prediction ($n_0 > 1$) is the same, except the task becomes increasingly more difficult for larger n_0. Prediction is widely applied in forecasting and modeling. The present research is concerned with forecasting damage. The forecasting problem may be simply formulated as follows: The damage distribution in the structure is known up to the present time n. The objective is to determine what the next damage state, $D(n+1)$, of the time series is going to be. The idea is that if a system can be trained to predict the former values (damage distribution states) of the time series (that is, if the time series for state $k < n$ is fed to the system and the request is to predict state $k+1$), then the system will also accurately predict state $n+1$. Figure 17 shows the block diagram to implement single-step prediction. The input is delayed by one sample/state before it is fed to the network. The desired output is the current state of the input $D(n)$. The input of the network is therefore delayed one sample with respect to the desired response.

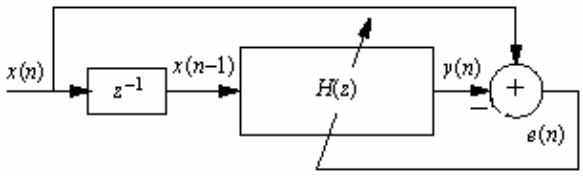

Figure 17 Block diagram to implement single-step prediction.

Numerical results are presented for progressive damage of an angle-ply, (45/-45/45), simply-supported plate subjected to a uniform load of 0.75 MPa, constant in time. The length and width of the laminate are 0.25m. The thickness of each ply is 0.6667mm, giving a total laminate thickness of h = 2mm and a length to thickness ratio of 125. The material used in the current study is M30/949 graphite/epoxy. The constituent properties of M30 carbon fibers and 949 epoxy are given in Table 6. Using these values for constituent properties and a fiber volume fraction of 60 percent, the damage evolution model was then applied to generate the values of stiffness reduction in the matrix at each grid point in the model area. These data were then transformed to time series of stiffness reductions at the different points in the model area that were identified with the Time Delay Neural Network (TDNN) based agents.

Representative grid points for the location of the TDNN-based agents were identified in the numerical model area and the time series of stiffness reductions at these points were prepared. In the first set of experiments the TDNN -based agent at each selected grid point received its input from present and previous values of the stiffness reductions of the nearest surrounding agents, which in turn could be associated with certain grid points. The agents then predicted the corresponding values of the variable at that point for the next time step. This also meant that stiffness reductions at the present and previous time steps of each selected grid point were passed as inputs to the TDNN agents of the nearest grid points to predict the stiffness reductions at the next time step at

those points. Typical verification results of this investigation are shown in Figs. 18 – 20 for one grid point in the model area. The size of the tap delay line is the variable that controls the size of the model, so it has to be experimentally determined. Larger models normally work better, but this depends on the type of data. For instance, larger models do not improve performance when the data (damage progression) is chaotic. Larger models simply utilize more information from the past to establish the value at the next time step.

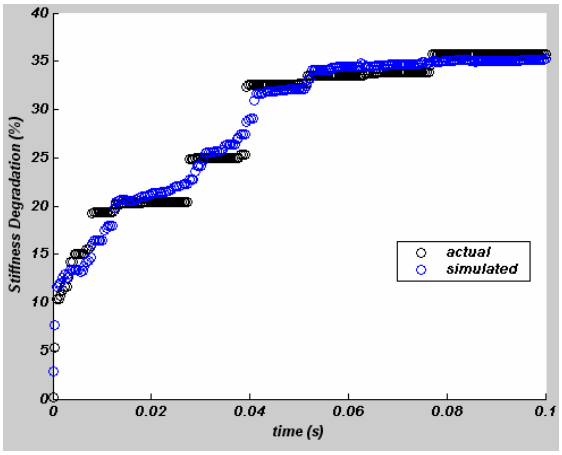

(a) Delay = 0.0012 s

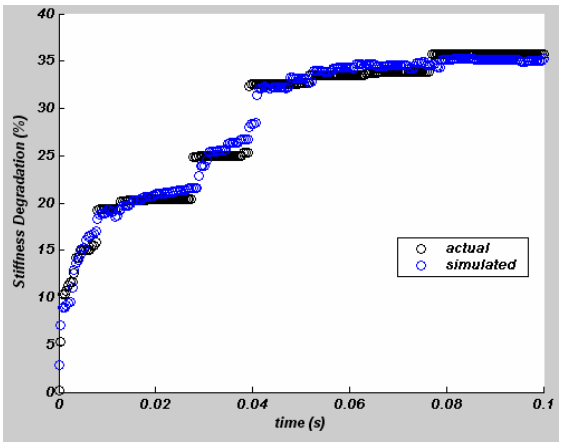

(b) Delay = 0.0044 s

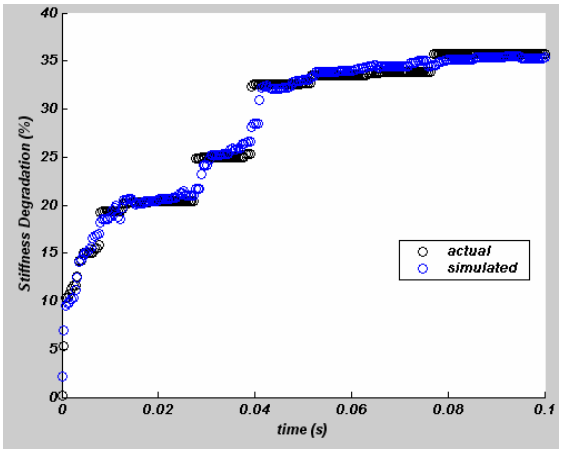

(c) Delay = 0.0064 s

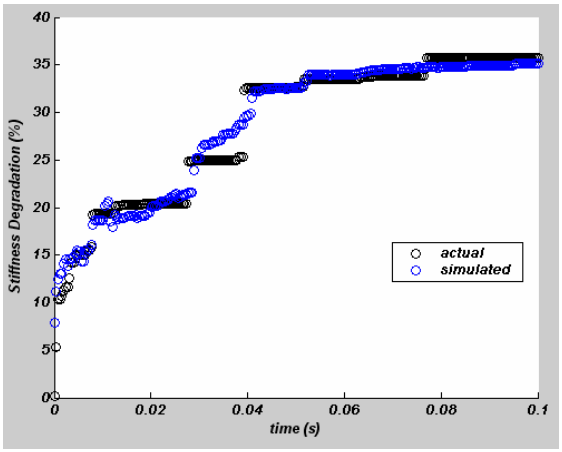

(d) Delay = 0.012 s

Figure 18 Damage (percentage reduction in matrix stiffness) evolution in the bottom layer of a (45/-45/45) simply-supported plate loaded by uniform tractions of 0.75MPa.

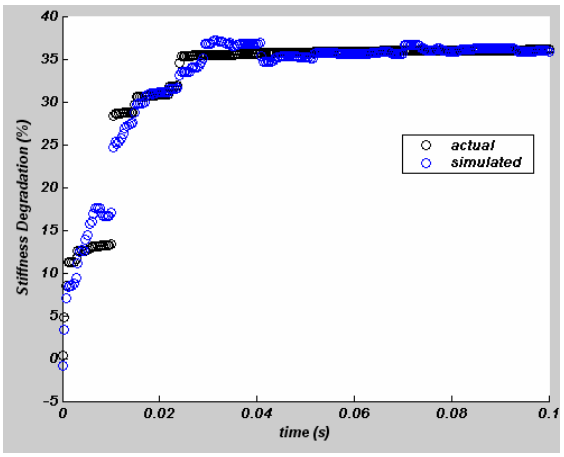

(a) Delay = 0.0012 s

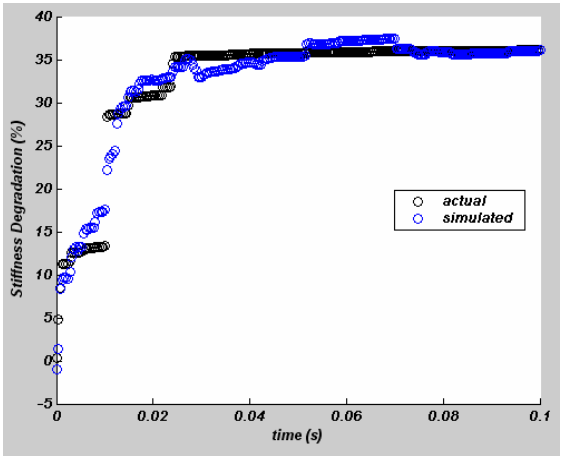

(b) Delay = 0.0044 s

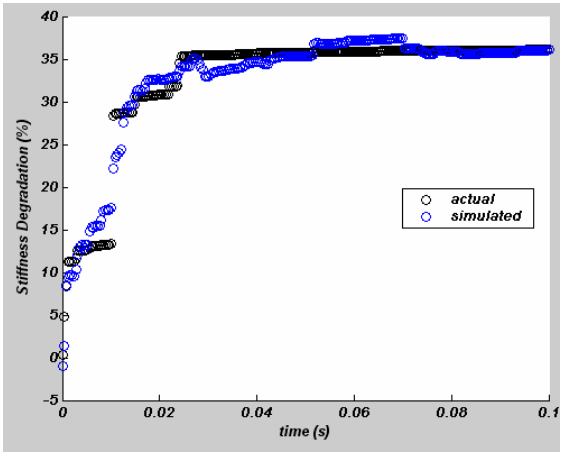

(c) Delay = 0.0044 s

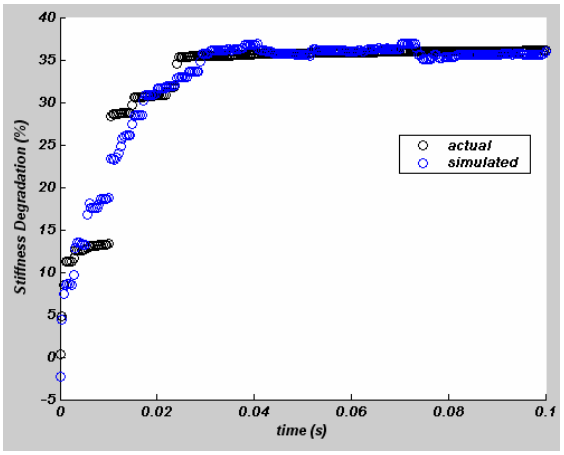

(d) Delay = 0.0064 s

Figure 19 Damage (percentage reduction in matrix stiffness) evolution in the middle layer of a (45/-45/45) simply-supported plate loaded by uniform tractions of 0.75MPa.

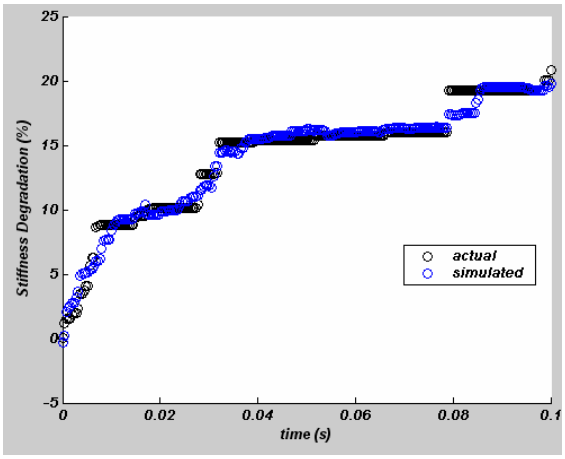

(a) Delay = 0.0012 s

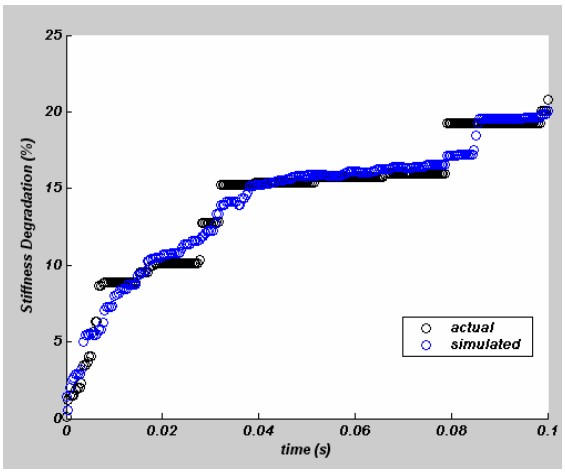

(b) Delay = 0.0028 s

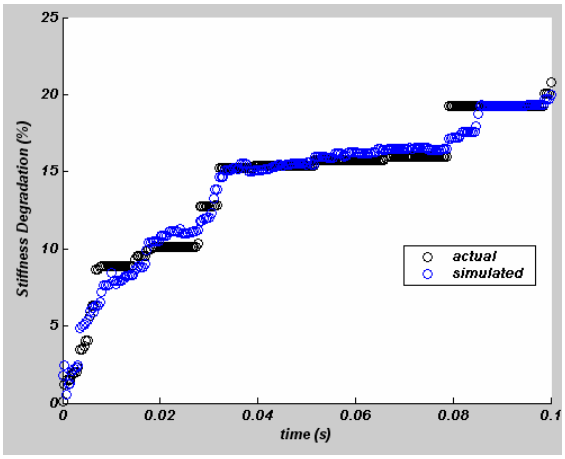

(c) Delay = 0.0036 s

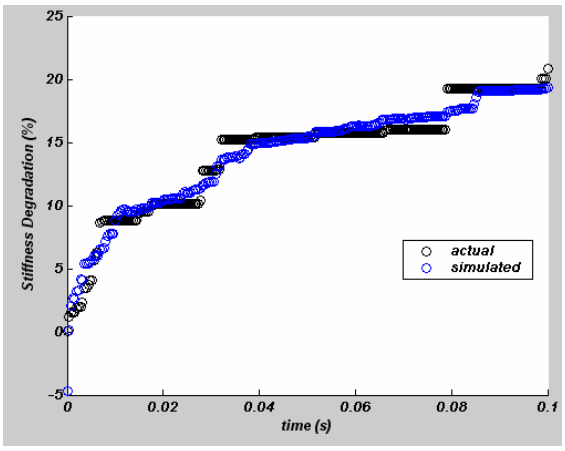

(d) Delay = 0.0044 s

Figure 20 Damage (percentage reduction in matrix stiffness) evolution in the top layer of a (45/-45/45) simply-supported plate loaded by uniform tractions of 0.75MPa.

But if the time series changes rapidly and it is aperiodic, this is of no help. Experimenting with the size of the delay line one can immediately see that this is true (Fig. 21).

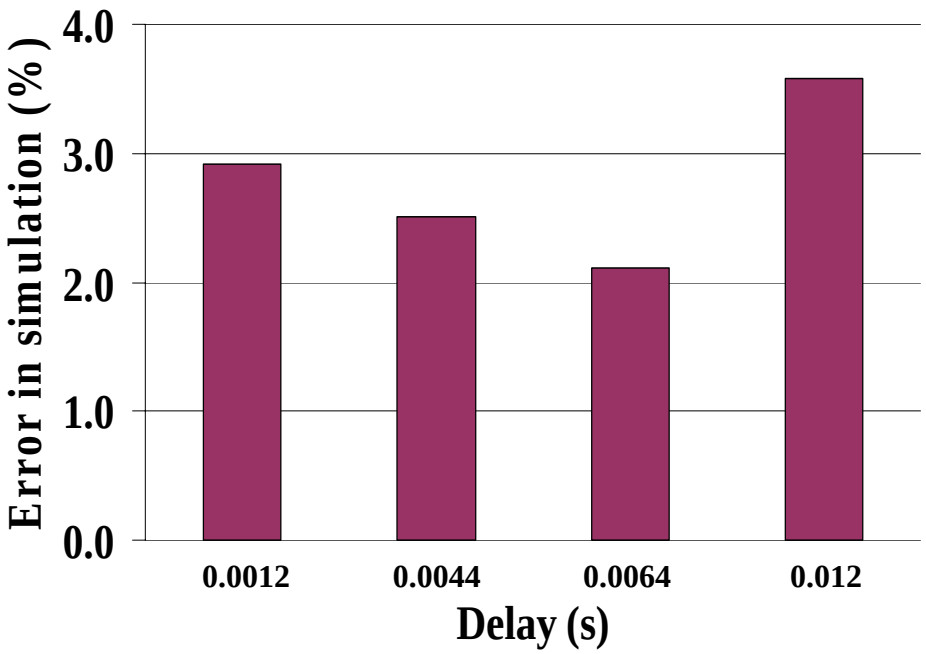

Figure 21 Influence of the delay line size on the accuracy of simulation.

A second set of experiments was performed in which multistep prediction (Fig. 22) was attempted by steadily increasing the lag between the desired response and the input. The accuracy drops rapidly for multistep prediction as may be seen in Fig. 23.

In general, the results of these two investigations show that agents constructed from TDNNs may be used as tools in the simulation of progressive damage in composite laminates effectively. But the conclusion is clearly highly restricted, since the experiments are specific to time delay neural networks. The next set of numerical experiments use agents composed exclusively of recurrent neural networks as non-linear dynamic system models to encapsulate progressive damage and to reproduce the temporal sequence of events observed in a model area.

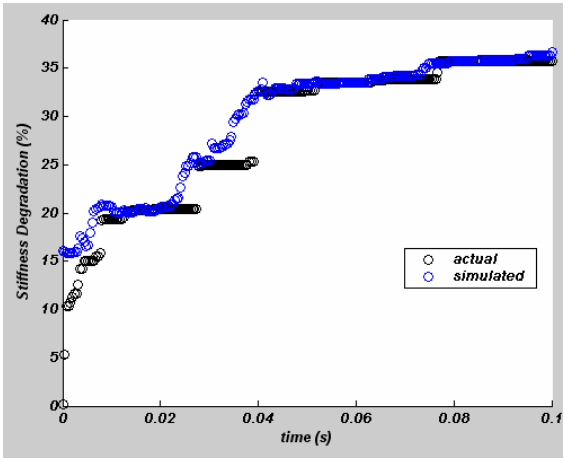

(a) Delay = 0.0012 s; Number of time steps predicted = 11

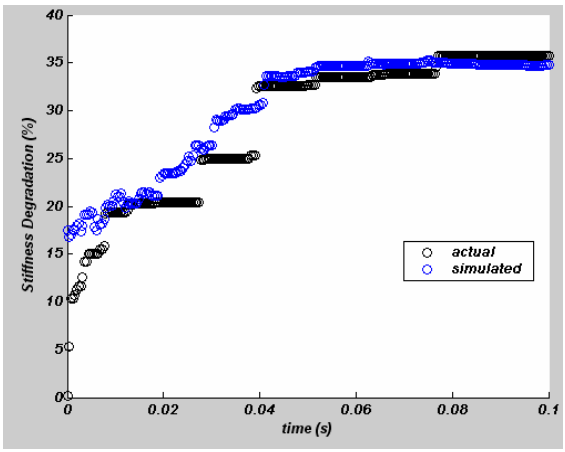

(b) Delay = 0.0012 s; Number of time steps predicted = 16

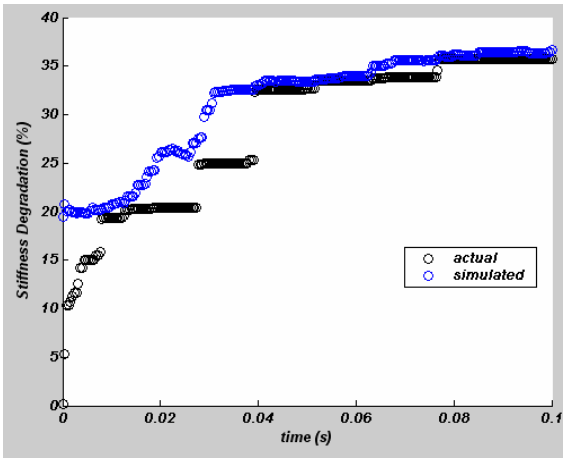

(c) Delay = 0.0012 s; Number of time steps predicted = 30

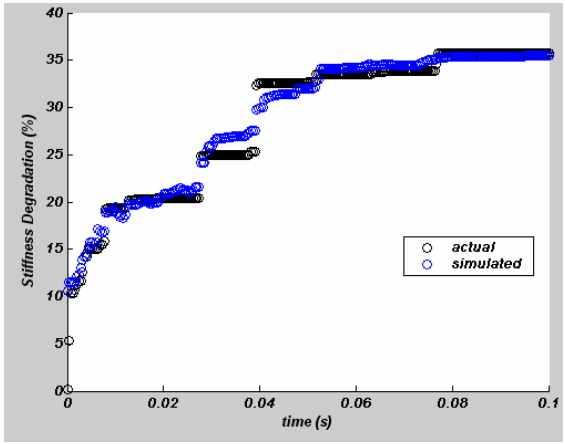

(d) Delay = 0.0064 s; Number of time steps predicted = 2

Figure 22 Multistep predictions.

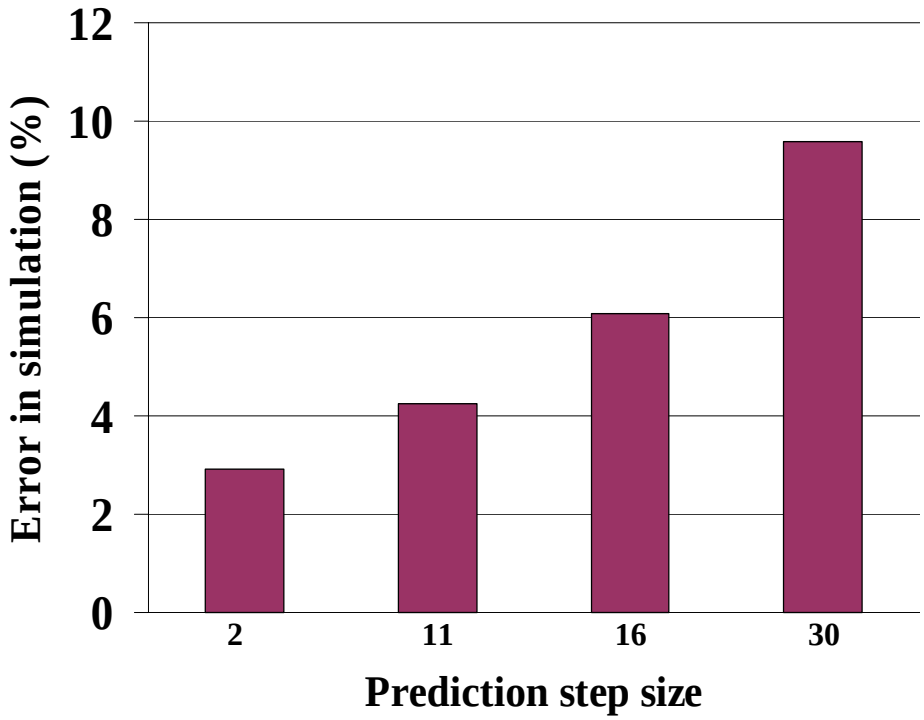

Figure 23 Effect of multistep prediction on accuracy of simulation.

As a first step, a somewhat modest experiment is undertaken. The goal is to diagnose the condition of a structure, described in terms of stiffness reduction. Diagnosing the structural degradation over time requires a physical inventory of the system response over the corresponding period. Such data may be collected as measurements of system response taken at a testing site or through a numerical simulation if a reliable model of the degradation process exists. The first example used in the verification of the response surface approach involves a simply-supported cross-ply (0/90/0) plate (Table 7) subjected to a variety of loading conditions. In practice, if the system responses under the more typically encountered load conditions are used to train the network, then field measurements of the system response would be sufficient to diagnose the health of the structure.

Table 7.
Plate dimensions and material specifications.

Length	0.25m
Width	0.25m
Ply thickness	0.6667mm
Total laminate thickness	2mm
Length/thickness	125
Material	M30/949 graphite/epoxy
Fiber volume fraction	60%

The previously discussed macro-micro finite element analysis program is used to generate sample data for the inverse mapping between structural degradation and the

transient response under a given load. The training data consists of a set of transient response curves and the corresponding damage evolution trajectories. The dynamic response curves correspond to a variety of excitations ranging in magnitude from 0.3 to 0.75 MPa, in behavior, from a constant function, through step, ramp, impulse, and sine functions, to a single cycle sine function.

In operation, the network should return an approximation of the degradation process when presented with some transient response curve at the input. The task is one of diagnosis, and a locally-recurrent architecture (Fig. 24) shows itself adequate to this type of task. Ideally, the neural diagnostic tool should generalize, that is, it should be able to reconstruct the trajectory of the damage progression when presented a transient response curve which the network has never seen before. Traditional knowledge from data modeling and recent developments in learning theory (Vapnik, 1995) clearly indicate that after a critical point the learning algorithm can over-fit the training data, resulting in poor performance on data not used in training. The current framework circumvents this problem by early stopping, or stopping with cross-validation – 10% of the training data is set aside for measuring training progress and at regular intervals (*i.e.*, 5 to 10 iterations), the network performance with the prevailing weights is tested against this data, called the cross-validation set; training is stopped at the point of maximum generalization, that is, when the error in the cross-validation set starts to increase (Fig. 1). The mean value of a relative error for cross-validation data is obtained as 2.1%. Such a low value clearly indicates that the network is capable of generalization. The test set used to verify the model performance consists of a combination of data from the training set and new/unseen data not used for training but for which the desired response is still known. Figure 25 shows a transient response curve used to test the network post-training and the corresponding damage progression trajectory, actual and simulated. Results of this simulation show that a relatively small network (7 neurons in the hidden layer) represents the mapping satisfactorily.

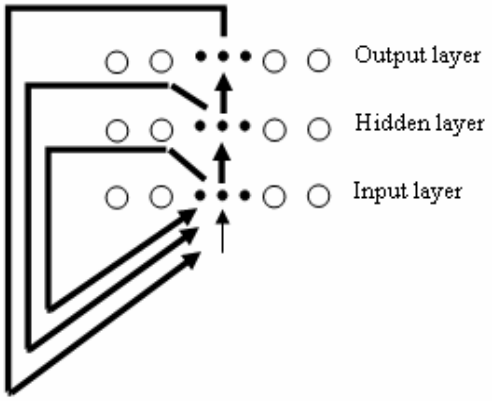

Figure 24 Locally-recurrent architecture.

The performance of the trained network is measured by performing a regression analysis between the network response and the corresponding targets. The correlation coefficient between the outputs and targets is a measure of how well the variation in the output is explained by the targets; if this number is equal to 1, there is perfect correlation between targets and outputs. In the example shown (Fig. 26), the number is very close to

1, which indicates a good fit. The mean value of a relative square error for training data is obtained as 12%.

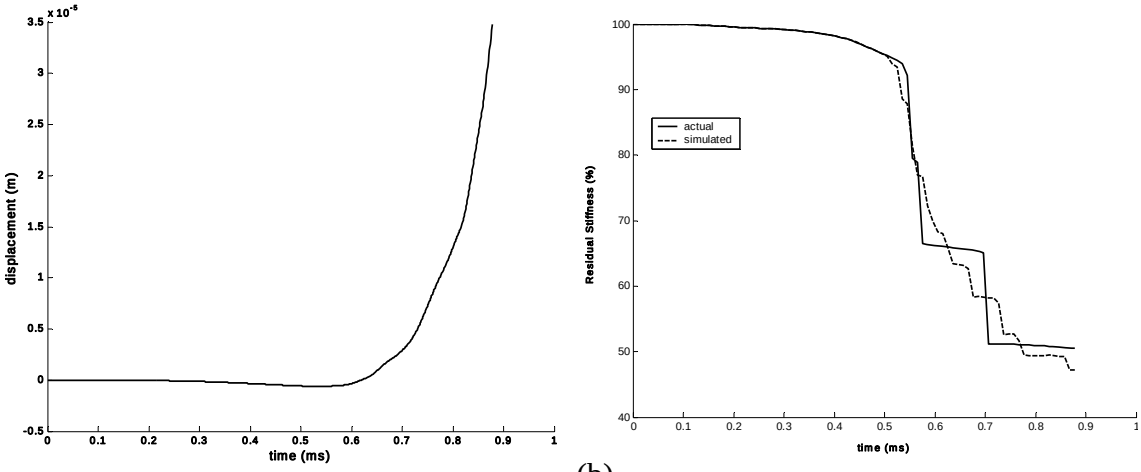

(a) (b)

Figure 25 (a) Transient response of a (0/90/0) simply-supported plate loaded by uniform tractions of 0.675MPa, (b) Comparison of neural-network-simulated damage evolution with finite element model results.

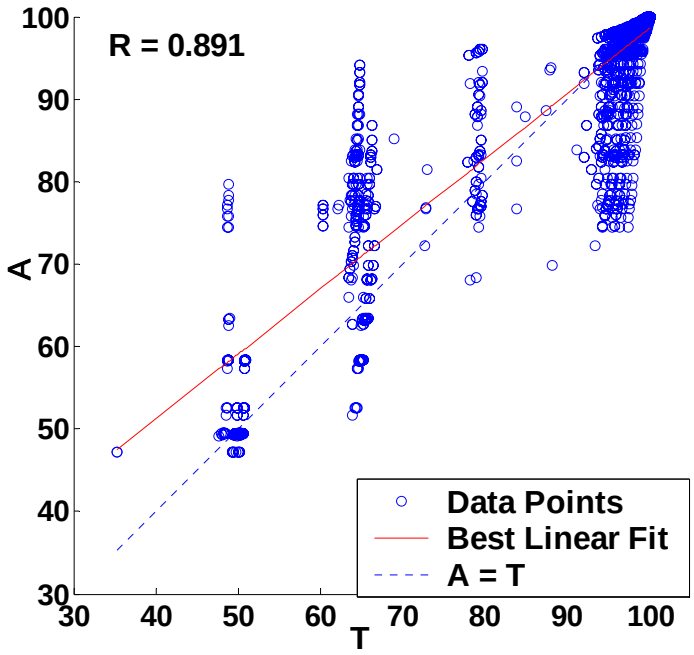

Figure 26 Quality of network training for first recurrent architecture.

The next task given to the network is to learn to predict the progression of damage, given a fragment of the damage progression stream. For this simulation a network similar to that in the first simulation is used, except that (1) intralayer connections in the input layers are eliminated, and (2) the basic network used in the previous simulation is expanded; the input and hidden layers contain 17 and 21 nodes, respectively. The training regimen involves presenting each damage state, one at a time, in sequence. The task for the network is to predict the next input. The sequence wraps

around, that the first state is presented after the last. The network is trained on 12000 passes through a sequence. It is then tested on another sequence that obeys the same regularities as a fragment of the original, but with noise added to the data. The actual and predicted evolutions are shown in Fig. 27. It is obvious that the error builds with time and the ability to predict correctly is quite poor.

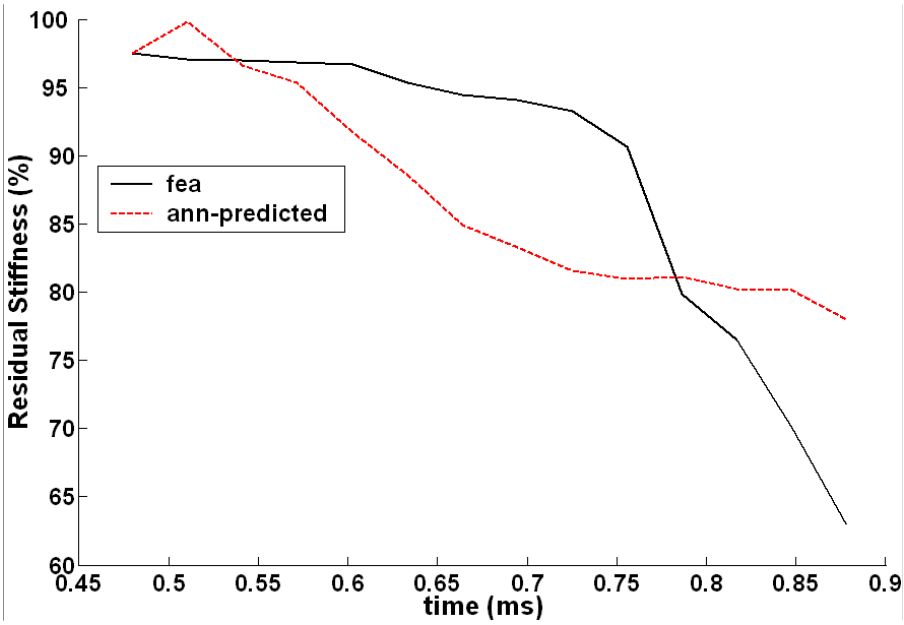

Figure 27 Comparison of neural prognostics of damage evolution with finite element model results.

A network should be able to work with incomplete and noisy input data. This feature seems to be particularly useful in the present application, as incomplete and noisy data are the rule rather than the exception in practical field tests involving structural systems. A training strategy for handling noise in data is devised as follows: To create a network that can handle noisy input data it is best to train the network on both ideal and noisy data. To do this, the network is first trained on ideal data for a maximum of 6000 epochs or until it has a low sum-squared error. Then, to obtain a network not sensitive to noise, the network is trained on two ideal copies and two noisy copies of the data. The noisy data has noise of mean 10% and 20% added to it. This forces the network to learn how to properly identify noisy data, while maintaining its ability to respond well to noise-free data. To train with noise, the maximum number of epochs is reduced to a small fraction of the number of epochs used during the previous stage of training and the error goal is increased, reflecting that higher error is expected given the nature of the sequence (more data sequences, including some with noise). The choice of number of epochs is determined heuristically. Once the network is trained with noise, it is again trained on just ideal data to ensure that it responds perfectly when presented with ideal data. The training strategy is summarized in Fig. 28.

The reliability of the neural network sequence reproduction system is measured by testing the network with fragments of the damage progression trajectory with varying quantities of noise. Figure 29 compares the network prognostics with the actual

degradation when noise of mean 5% is added to the fragment presented to the network. It is obvious that training the network on noisy input data greatly reduces its errors when it

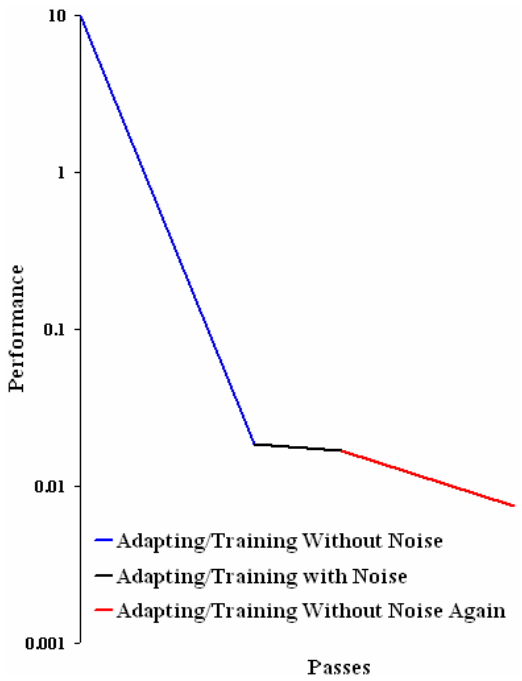

Figure 28 A training strategy for handling noise in data.

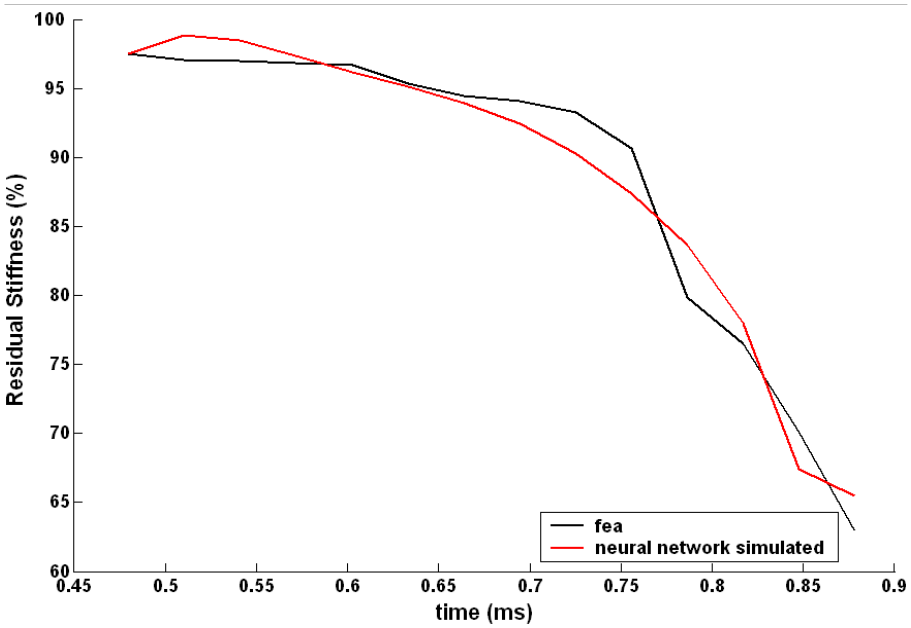

Figure 29 Comparison of neural prognostics of damage evolution with finite element model results.

has to work with noisy data. If a higher accuracy is needed, the network can be trained for a longer time or retrained after decreasing network resolution or increasing the size of

the network. As a final comment, it is indicated that the reliability of network approximations could be further heightened to handle higher levels of noise by training it on input data with greater amounts of noise.

Numerical results are also presented for progressive damage of angle-ply, (30/-60/30), (45/-45/45), plates subjected to a uniform load of 0.75 MPa, constant in time. The time scale over which damage effects first make their appearance in the cross-ply laminate is shorter relative to the angle-ply laminates. The system response is studied over a period of 0.88 ms and the plot of the temporal evolution of the damage parameter (Fig. 29) reveals a dramatic perturbation in the stiffness of the matrix in the top ply post the 0.5-ms mark. An obvious factor that contributes to this dramatic perturbation is the heightened stiffness of the cross-ply laminate. This is in contrast to the response of the two angle-ply laminates (Figs. 30 and 31) in which most of the damage is nucleated within 50 ms from the time when the structure is loaded. The damage evolution stabilizes i.e., the maximum perturbation does not seem to increase appreciably over the remaining time post the 50-ms mark, but the region of damage spreads and eventually the clusters may coalesce to form larger clusters thereby raising the specter of complete failure. The system response is studied over a broader temporal scale (100 ms) relative to the cross-ply laminate. For this reason, the angle-ply damage trajectories are easier to learn and predict and the network could be trained with fewer neurons (9) in its hidden layer with no significant increase in the error of the network approximations. Figures 30 and 31 furnish proof of same.

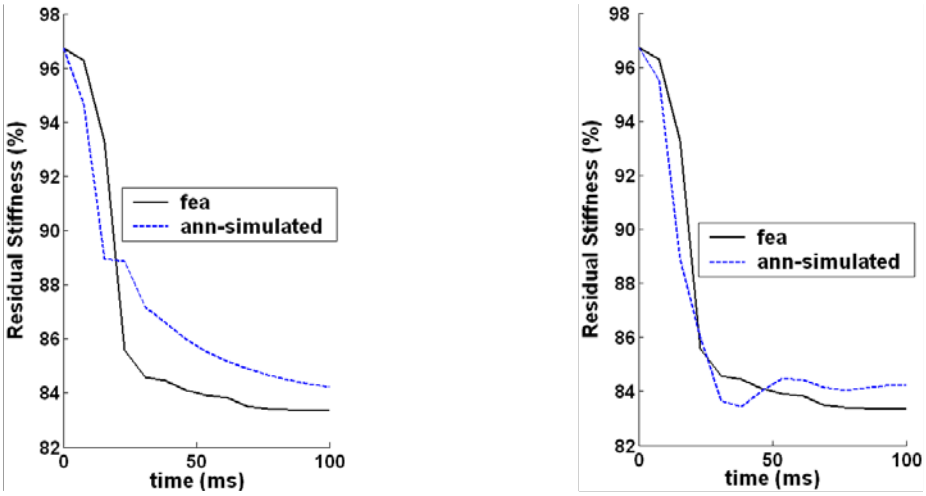

Figure 30 Comparison of neural prognostics of damage evolution in a (30/-60/30) plate with FEM results when the network has (a) not been trained to handle noisy data, (b) been trained to handle noisy data.

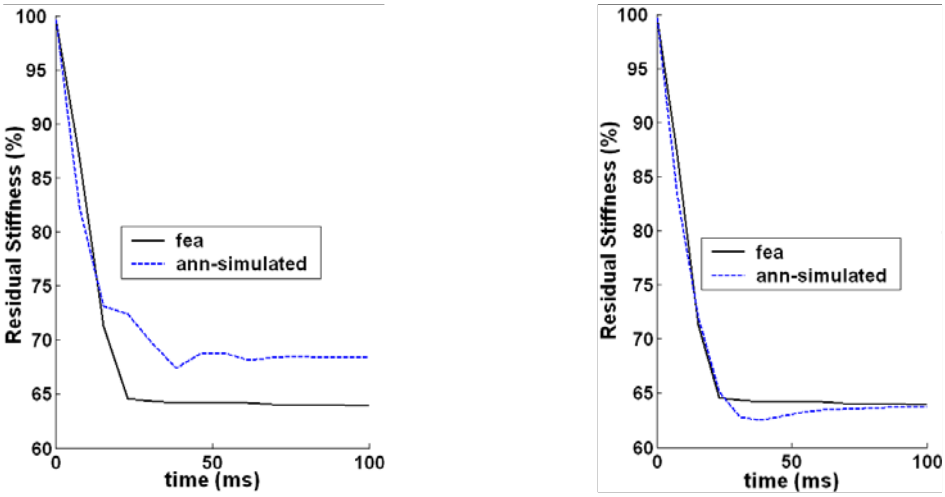

Figure 31 Comparison of neural prognostics of damage evolution in a (45/-45/45) plate with FEM results when the network has (a) not been trained to handle noisy data, (b) been trained to handle noisy data.

One question which might be asked is whether the memory capacity of the response surface topology employed here can supply reliable diagnostics when it encounters inputs beyond its adaptive scope or outside its range of 'experience'. Two input sequences (Figs. 32 (a) and 33 (a)) are devised which are intended to address these scenarios. These are the transient responses to excitations, constant with time, of 0.77 MPa and 0.8 MPa, respectively. The corresponding degradation signals are shown in Figs. 32 (b) and 33 (b). The mean values of the relative square error estimates are 2.3% and 2.5%, respectively. This global error does not tell the whole story, however. The error signals for this testing phase are shown in Fig. 34. It is obvious that the error oscillates markedly; at some points in time, the diagnosis is correct and error is low, while at other points in time, the ability to diagnose correctly is quite poor. More precisely, error tends to be high when the network encounters outliers, points which are abnormally far from the response surface domain. The farthest outliers encountered by the model when it is presented the input sequences shown in Figs. 32 (a) and 33 (a) are, respectively, approximately 11% and 32% greater relative to the upper bound of the domain. To verify the accuracy of the response model, the response surface solutions are compared with direct FE analysis solutions at these locations in the input space. The relative squared errors are, respectively, 0.1% and 10%. Errors stemming from data or behavior outside the response surface space (area encircled in blue in Fig. 34) should not be confused with diagnostic errors which might result from data within the mapping space (area encircled in green in Fig. 34). The latter are associated with the learning process and the accuracy of the mapping can be refined through longer training times and/or increased processing and memory requirements. This simulation demonstrates that to improve diagnostics from a quantitative standpoint, it is necessary to develop a response surface topology that is comprehensive enough to reflect as complete a scope of the load conditions as is realistically possible.

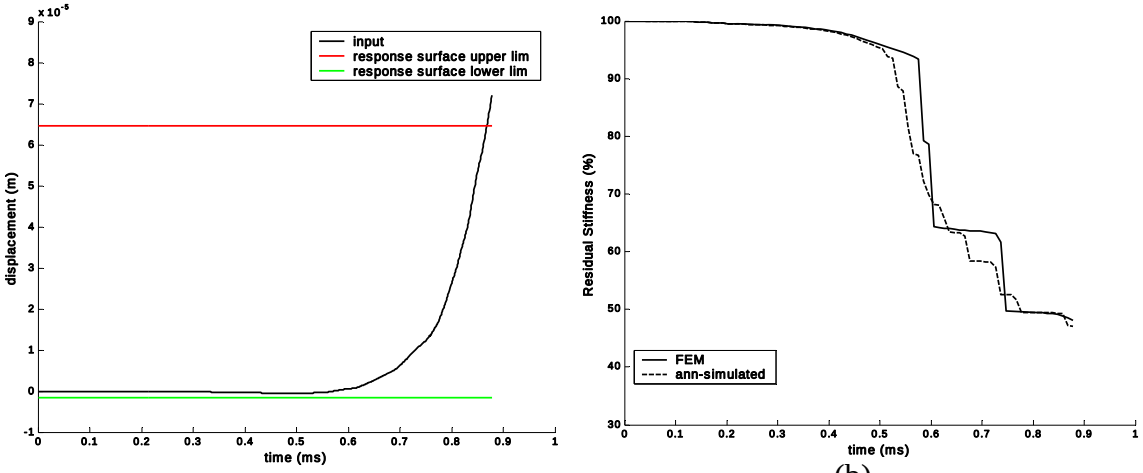

(a) (b)

Figure 32 (a) Transient response of a (0/90/0) simply-supported plate loaded by uniform tractions of 0.77 MPa, (b) Comparison of ANN-simulated damage evolution with FE analysis results.

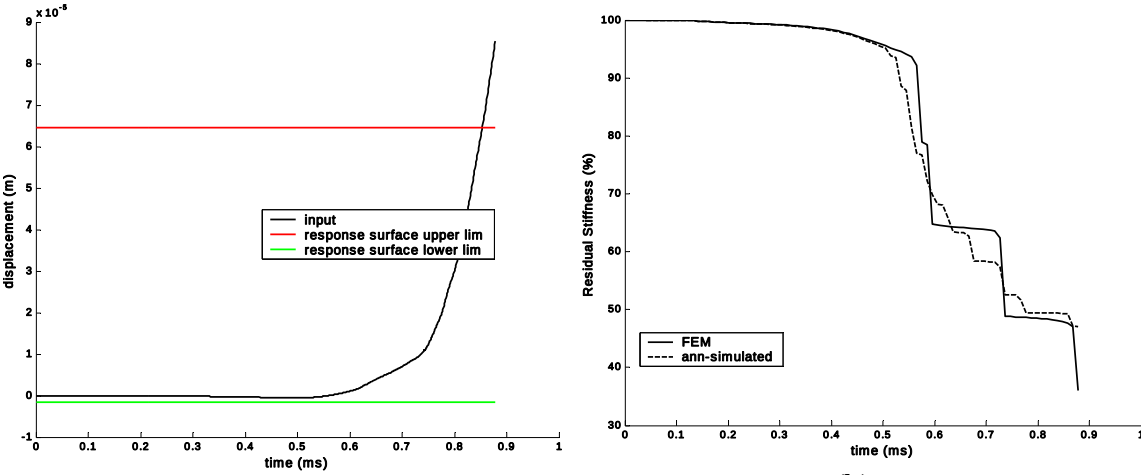

(a) (b)

Figure 33 (a) Transient response of a (0/90/0) simply-supported plate loaded by uniform tractions of 0.8 MPa, (b) Comparison of ANN-simulated damage evolution with FE analysis results.

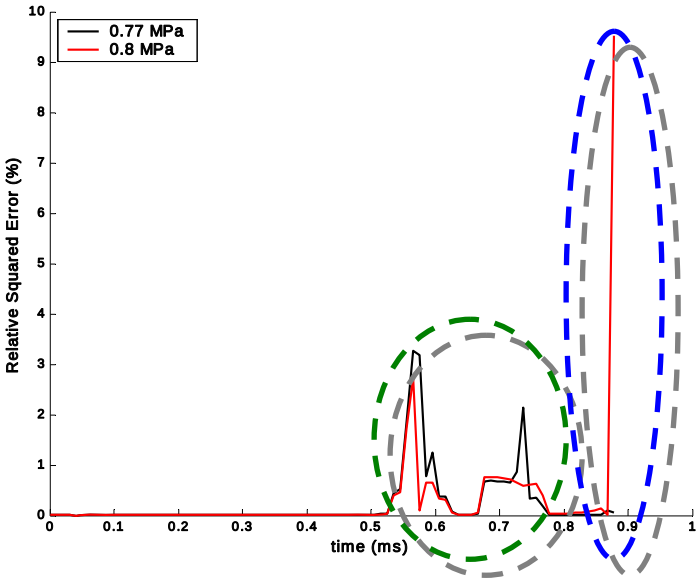

Figure 34 Graph of error relative to FE analysis solution in temporal association task.

PUBLICATIONS

Deenadayalu, C. A., Chattopadhyay, A. and Goldberg, R. K, "General Formulation for Basic Mechanical State Equations of Fatigue-Damage Process in Laminate Composites," To be presented at *AIAA/ASME/ASCE/AHS/ASC 48th Structures, Structural Dynamics and Materials Conference*, AIAA, Honolulu, HI, 2007.

Deenadayalu, C. A., Chattopadhyay, A. and Zhou, X., "Application of Artificial Neural Networks to the Simulation of Progressive Damage in Composite Laminates," *AIAA/ASME/ASCE/AHS/ASC 47th Structures, Structural Dynamics and Materials Conference*, AIAA, Newport, RI, 2006.

Deenadayalu, C. A., Chattopadhyay, A. and Zhou, X., "Constitutive Modeling of Progressive Damage in Composite Laminates," *AIAA/ASME/ASCE/AHS/ASC 46th Structures, Structural Dynamics and Materials Conference*, AIAA, Austin, TX, 2005.

Le, H., Chen, H. P. and Chattopadhyay, A., "Multiple and Generalized Delamination Detections Using Neural Network Technique and Genetic Algorithm," *Proceedings of the46th AIAA/ASME/ASCE/AHS/ASC Structures, Structural Dynamics and Materials Conference*, 2005.

Chen, H. P. and Kim, J., "A Combined Technique of Genetic Algorithms and Neural Networks for Delamination Detection in Composite Laminates," The Fifth Canadian International Composites Conference, CANCOM 2005, Vancouver, Canada, 2005.

Deenadayalu, C. A., Chattopadhyay, A. and Chen, H. P., "Characterization and Detection of Delamination in Composite Laminates Using Artificial Neural Networks," *Structural Health Monitoring Journal*, Article in press.

Deenadayalu, C. A., Chattopadhyay, A. and Chen, H. P., "Characterization and Detection of Delamination in Composite Laminates Using Artificial Neural Networks," Presented at *AIAA MDO Conference,* Albany, NY, 2004.

Chen, H. P., Le, H., Kim, J. and Chattopadhyay, A. "Delamination Detection Problems using a Combined Genetic Algorithm and Neural Network Technique," *Proceedings of* the *10th AIAA/ISSMO Multidisciplinary Analysis and Optimization Conference*, Albany, New York, 2004.

BIBLIOGRAPHY

Aboudi, J.A., 1991. Mechanics of Composite Materials: A Unified Micromechanical Approach. Elsevier, Amsterdam.

Aboudi, J.A., 1995. Micromechanical analysis of therino-inelastic multiphase short-fiber composite. Composite Engineering 5(7), 839-850.

Aboudi, J.A., 1989. Micromechanical analysis of composites by the method of cells. Applied Mechanics Review 42, 193-221.

Agarwal, B.D., Broutman, L.J., 1990. Analysis and Performance of Fiber Composites. John Wiley and Sons, New York.

Ambartsumyan, S.A., 1969. Theory of Anisotropic Plates. Translated from Russian by Cheron, T. Technomic, Stamford, CT.

Araújo, A.F.R., D'arbo Jr, H., 1997. The role played by intralayer and interlayer feedback connections in recurrent neural networks used for planning. Journal of the Brazilian Computer Society 4(1), 38-49.

Araújo, A.F.R., D'Arbo Jr., H., 1998. A Partially Recurrent Neural Network to Perform Trajectory Generation, Inverse Kinematics, and Inverse Dynamics. Proceedings of the 1998 IEEE International Conference on Systems, Man, and Cybernetics, San Diego, Ca., 1784-1789.

Araújo, A.F.R., D'Arbo Jr., H., 1998. Partially Recurrent Neural Networks for Production of Temporal Sequences. Proceedings of the 1998 IEEE International Joint Conference on Neural Networks, Anchorage, Ak., 474-479.

Argyris, J., Mlejnek, H.P., 1991. Dynamics of Structures. North-Holland, Amsterdam.

Avery, W.B., Herakovich, C.T., 1986. Effect of fiber anisotropy on thermal stresses in fibrous composites. Journal of Applied Mechanics 53(4), 751-756.

Banks-Sills, L., Leiderman, V., and Fang, D.N., 1997. On the effect of particle shape and orientation on elastic properties of metal matrix composites. Composites, Part B 28 (4), 465-481.

Barai, S.V., Pandey, P.C., 1994. Vibration signature analysis using artificial neural networks. Journal of Computing in Civil Engineering 9(4), 259-265.

Barbero, E.J., De Vivo, L., 2001. A constitutive model for elastic damage in fiber-reinforced PMC laminae. International Journal of Damage Mechanics 10, 73-93.

Bathe, K.J., 1996. Finite Element Procedures. Prentice Hall, Englewood Cliffs, NJ.

Belytschko, T., Liu, W.K., Moran, B., 2000. Nonlinear Finite Elements for Continua and Structures. John Wiley & Sons Ltd. Chichester, West Sussex, England.

Bodner, S. R., 2002. Unified Plasticity for Engineering Applications. Kluwer Academic/Plenum Publishers, New York.

Box, G.E.P., Draper, N.R., 1987. Empirical Model Building and Response Surfaces. John Wiley and Sons, Inc., New York.

Carrera, E., 1998. Evaluation of layerwise mixed theories for laminated plates analysis. AIAA Journal 36(5), 830-839.

Chandrupatla, T.R. Belegundu, A.D., 2002. Introduction to Finite Elements in Engineering. Prentice Hall, Upper Saddle River, NJ.

Chang, F.K., Chang, K.Y., 1987a. A progressive damage model for laminated composites containing stress concentrations. Journal of Composite Materials 21(9), 834-855.

Chang, F.K., Chang, K.Y., 1987b. Post-failure analysis of bolted composite joints in tension or shear-out mode failure. Journal of Composite Materials 21(9), 809-833.

Chattopadhyay, A., Gu H., 1994. New higher-order plate theory in modeling delamination buckling of composite laminates. AIAA Journal 32(8) 1709-1716.

Chattopadhyay, A., Nam, C., Dragomir-Daescu, D., 1999. Delamination modeling and detection in smart composite plates. Journal of Reinforced Plastics and Composites 18(17), 1557-1572.

Chen, H.P., Karunaratne, R., 2002. Optimum Stacking Sequence Design of Composite Laminates using Genetic Algorithms. 47th International SAMPE Symposium, Long Beach, Ca., 1402-1414.

Chen, H.P., Karunaratne, R., 2002. “Study of Optimal Composite Layup Design Using Enhanced GA”, Ninth International Conference on Composites Engineering, San Diego, California.

Chen, H.P., Le, H., Kim, J., Chattopadhyay, A., 2004. Delamination Detection Problems Using a Combined Genetic Algorithm and Neural Network Technique. 10th AIAA/ISSMO Multidisciplinary Analysis and Optimization Conference, AIAA-2004-4397, Albany, NY.

Chen, H.P., Kim, J., 2005. “A Combined Technique of Genetic Algorithms and Neural Networks for Delamination Detection in Composite Laminates,” The Fifth Canadian International Composites Conference, CANCOM 2005, in Vancouver, Canada.

Chipperfield, A.J., Fleming, P.J., Fonseca, C.M., 1994. Genetic Algorithm Tools for Control Systems Engineering. Proceedings of the Adaptive Computing in Engineering Design and Control, Plymouth Engineering Design Centre, 128-133.

Chipperfield, A.J., Fleming, P.J., 1995. The MATLAB® Genetic Algorithm Toolbox. Proceedings of the IEE Colloquium on Applied Control Techniques Using MATLAB®.

Cook, R.D., Malkus, D.S., Plesha, M.E., 1989. Concepts and Applications of Finite Element Analysis (3rd Edition). John Wiley, NY.

Daniel, I.M., Ishai, O., 2006. Engineering Mechanics of Composite Materials. Oxford Universtiy Press, New York, New York.

De Jong, K., 1975. An Analysis of the Behavior of a Class of Genetic Adaptive Systems. Doctoral Thesis. University of Michigan.

Demuth, H., Beale, M., 2003. Neural Network Toolbox – for Use with MATLAB®. User's Guide, Version 4, MathWorks Inc..

Dibike, Y.B., Abbott, M.B., 1999. Application of artificial neural networks to the simulation of a two dimensional flow. Journal of Hydraulic Research 37(4), 435-446.

Disciuva, M., 1987. An improved shear-deformation theory for moderately thick multilayered anisotropic shells and plates. Journal of Applied Mechanics-Transactions of the ASME. 54 (3), 589-596.

Doebling, S.W., Farrar, C.R., Prime, M.B., Shevitz, D. W., 1996. Damage Identification and Health Monitoring of Structural and Mechanical Systems from Changes in Their Vibration Characteristics: A Literature Review. Los Alamos National Laboratory Report LA-13070-MS, Los Alamos, NM.

Dong, S.B., Pister, K.S., Taylor, R.L., 1962. On the theory of laminated anisotropic shells and plates. Journal of Aeronautical Science 29 (8), 969-975.

Draper, N.R., Smith, H., 1981. Applied Regression Analysis. John Wiley and Sons, Inc., New York.

Dvorak, G.J., 1991. Plasticity theories for fibrous composite materials. Metal Matrix Composites: Mechanisms and Properties. Academic Press, Boston, 1-77.

Elman, J.L., 1990. Finding structure in time. Cognitive Science 14, 179-211.

Eshelby, J.D., 1957. The Determination of the Elastic Field of an Ellipsoidal Inclusion, and Related Problems. Proceedings of the Royal Society of London Series A-Mathematical and Physical Sciences 241 (1226), 376-396.

Flugge, W., 1967. Stresses in Shells. Springer-Verlag, New York.

Friswell, M.I., Penny, J.E.T., Gravey, S.D., 1998. A combined genetic and eigensensitivity algorithm for the location of damage in structures. Computers and Structures 69, 547-556.

Goldberg, D.E., Deb, K., 1991. A Comparative Analysis of Selection Schemes used in Genetic Algorithms, Foundation of Genetic Algorithms. Ed. G.J.E. Rawlins (San Mateo, CA: Morgan Kaufmann), 69-93.

Goldberg R.K., 2001. Implementation of Fiber Substructuring Into Strain Rate Dependent Micromechanics Analysis of Polymer Matrix Composites. NASA/TM-2001-210822, National Aeronautics and Space Administration, Washington, D.C.

Goldberg, R.K, 1999. Strain Rate Dependent Deformation and Strength Modeling of a Polymer Matrix Composite Utilizing a Micromechanics Approach. NASA/TM-1999-209768, National Aeronautics and Space Administration, Washington, D.C.

Goldberg, R.K., 2000. Implementation of Laminate Theory Into Strain Rate Dependent Micromechanics Analysis of Polymer Matrix Composites. NASA/TM-2000-210351, National Aeronautics and Space Administration, Washington, D.C..

Goldberg, R.K., Roberts, G.D., Gilat, A., 2003. Implementation of an Associative Flow Rule Including Hydrostatic Stress Effects Into the High Strain Rate Deformation Analysis of Polymer Matrix Composites. NASA/TM-2003-212382, National Aeronautics and Space Administration, Washington, D.C..

Goldberg, R.K., Roberts, G.D., Gilat, A., 2003. Implementation of an Associative Flow Rule Including Hydrostatic Stress Effects Into the High Strain Rate Deformation Analysis of Polymer Matrix Composites. NASA/TM-2003-212382, National Aeronautics and Space Administration, Washington, D.C..

Goldberg, R.K., Roberts, G.D. and Gilat, A., 2004. Analytical Studies of the High Rate Tensile Response of a Polymer Matrix Composite. Journal of Advanced Materials 36(3), 14-24.

Goldberg, R.K, 1999. Strain Rate Dependent Deformation and Strength Modeling of a Polymer Matrix Composite Utilizing a Micromechanics Approach. NASA/TM-1999-209768, National Aeronautics and Space Administration, Washington, D.C..

Goldberg, R.K., Hopkins, D.A., 1995. Application of the boundary element method to the micromechanical analysis of composite materials. Computers and Structures 56 (5), 721-731.

Gu, H.Z., Chattopadhyay, A., 1996. Delamination buckling and postbuckling of composite cylindrical shells. AIAA Journal 34 (6), 1279-1286.

Hajela, P., Berke, L., 1991. Neurobiological computational models in structural analysis and design. Computers and Structures 41(4), 657-667.

Harrison, C., Butler, R., 2001. Locating delaminations in composite beams using gradient techniques and genetic algorithm. AIAA Journal 39(7), 1383-1389.

Hayakawa, K., Murakami, S., 1997. Thermodynamical modeling of elastic-plastic damage and experimental validation of damage potential. International Journal of Damage Mechanics 6, 332-362.

Hayakawa, K., Murakami, S., 1998. Space of Damage Conjugate Force and Damage Potential of Elastic-Plastic-Damage Materials. Damage Mechanics in Engineering Materials, Eds. G.Z. Voyiadjis, J.-W.W. Ju, J.-L. Chaboche, Elsevier Science, Amsterdam, 27-44.

Hayhurst, D.R., Trampczynski, W.A., Leckie, F.A., 1980. Creep Rupture under Non-Proportional Loading. Acta Metallurgica 28, 1171-1183.

Haykin, S., 1999. Neural networks: A comprehensive foundation (2nd ed.). Prentice Hall.

Haykin, S., Principe, J., 1998. Dynamic modeling with neural networks. IEEE Signal Processing Magazine 15(3), 66.

Hertz, J.A., Krogh, A., Palmer, R.G., 1991. Introduction to the Theory of Neural Computation, Addison-Wesley Publishing Company, Reading, Mass.

Hill, R., 1950. The Mathematical Theory of Plasticity. Oxford University Press, London.

Hinton, M.J., Kaddour, A.S., Soden, P.D., 2002. A comparison of the predictive capabilities of current failure theories for composite laminates, judged against experimental evidence. Composites Science and Technology 62 (12-13), 1725-1797.

Hsu, Y.S., Reddy, J.N., Bert, C.W., 1981. Thermoelasticity of circular cylindrical-shells laminated of bimodulus composite-materials. Journal of Thermal Stresses 4 (2), 155-177.

Jordan, M.I., 1989. Serial Order: A Parallel Distributed Approach. Advances in Connectionist Theory: Speech, Eds. J. L. Elman and D. E. Rumelhart, Erlbaum.

Kachanov, L.M., 2004. Fundamentals of the Theory of Plasticity. Dover Publications, Inc., New York.

Kant, T., Arora, C.P., Varaiya, J.H., 1992. Finite-element transient analysis of composite and sandwich plates based on a refined theory and a mode superposition method. Composite Structures 22 (2), 109-120.

Kant, T., Khare, R.K., 1994. Finite-element thermal-stress analysis of composite laminates using a higher-order theory. Journal of Thermal Stresses 17 (2), 229-255.

Kant, T., Kommineni, J.R., 1994. Geometrically nonlinear transient analysis of laminated composite and sandwich shells with a refined theory and c0 finite-elements. Computers and Structures 52 (6), 1243-1259.

Kant, T., Mallikarjuna, 1991. Nonlinear dynamics of laminated plates with a higher-order theory and c^o finite-elements. International Journal of Non-Linear Mechanics 26 (3-4), 335-343.

Kant, T., Ravichandran, R.V., Pandya, B.N. et al., 1988. Finite-element transient dynamic analysis of isotropic and fiber reinforced composite plates using a higher-order theory. Composite Structures 9(4), 319-342.

Kant, T., Varaiya, J.H., Arora, C.P., 1990. Finite-element transient analysis of composite and sandwich plates based on a refined theory and implicit time integration schemes. Computers & Structures 36 (3), 401-420.

Kapania, R.K., Raciti, S., 1989. Recent advances in analysis of laminated beams and plates: part i: shear effects and buckling. AIAA Journal 27 (7), 923-934.

Khan, A.S., Huang, S., 1995. Continuum Theory of Plasticity. John Wiley and Sons, Inc., New York.

Khdeir, A.A., Rajab, M.D., Reddy, J.N., 1992. Thermal effects on the response of cross-ply laminated shallow shells. International Journal of Solids and Structures 29 (5), 653-667.

Khdeir, A.A., Reddy, J.N., 1991. Thermal stresses and deflections of cross-ply laminated plates using refined plate theories. Journal of Thermal Stresses 14 (4), 419-438.

Kim, H.S., Chattopadhyay, A., Ghoshal, A., 2003. Dynamic Analysis of Cross-ply Composite Laminates with Embedded Multiple Delamination. AIAA/ASME/ASCE/AHS/ASC 44th Structures, Structural Dynamics and Materials Conference, AIAA, Norfolk, VA.

Kim, H.S., Zhou, X., Chattopadhyay, A., 2001. Interlaminar stress analysis of shell structures with piezoelectric patch including thermal loading. AIAA Journal 40(12), 2517-2525.

Kirchhoff, G., 1850. Uber das gleichgewicht und die bewegung einer elastischen scheibe. Reine und Angewante Mathematik (Crelle) 40, 51-88.

Klenke, S.E., Paez, T.L., 1996. Damage Identification with Probabilistic Neural Networks. Proceedings of the 14th International Modal Analysis Conference, Dearborn, MI.

Knott, T.W., Herakovich, C.T., 1988. Effect of Fiber Morphology on Composite Properties. CCMS-88-09, VPI-E-88-16, Virginia Tech, Blacksburg.

Knott, T.W., Herakovich, C.T., 1991. Effect of fiber orthotropy on effective composite properties. Journal of Composite Materials 25 (6), 732-759.

Kommineni, J.R., Kant, T., 1993. Large deflection elastic and inelastic transient analyses of composite and sandwich plates with a refined theory. Journal of Reinforced Plastics and Composites 12 (11), 1150-1170.

Kuraishi, A., Tsai, S.W., Liu, K., 2002. A progressive quadratic failure criterion. Composites Science and Technology 62 (12-13), 1683-1695.

Le Riche, R., Haftka, R.T. 1995. Improved genetic algorithm for minimum thickness composite laminate design. Composites Engineering 5(2), 143-161.

Li, F.Z; and Pan, J., 1990. Plane-stress crack-tip fields for pressure-sensitive dilatant materials. Journal of Applied Mechanics 57 (1), 40-49.

Librescu, L., 1975. Elastostatics and Kinetics of Anisotropic and Heterogeneous Shell-type Structures. Noordhoff, Leyden, Netherlands.

Mallikarjuna, Kant, T., 1990. Finite-element transient-response of composite and sandwich plates with a refined higher-order theory. Journal of Applied Mechanics-Transactions of the ASME 57 (4), 1084-1086.

Mallikarjuna, Kant, T., 1993. A critical review and some results of recently developed refined theories of fiber-reinforced laminated composites and sandwiches. Composite Structures 23 (4), 293-312.

Mindlin, R.D., 1951. Influence of rotatory inertia and shear on flexnral motions of isotropic, elastic plates. Journal of Applied Mechanics, Transactions of ASME 18, 31-38.

Mital, S.K., Murthy, P.L.N., Chamis, C.C., 1995. Micromechanics for ceramic matrix composites via fiber substructuring. Journal of Composite Materials 29 (5), 614-633.

Moller, M.F., 1993. A scaled conjugate gradient algorithm for fast supervised learning. Neural Networks 6, 525-533.

Murakami, S., Kamiya, K., 1997. Constitutive and damage evolution equations of elastic-brittle materials based on irreversible thermodynamics. International Journal of Mechanical Sciences 39(4), 473-486.

Naboulsi, S.K., Palazotto, A.N., 2003. Non-linear static-dynamic finite element formulation for composite shells. International Journal of Non-Linear Mechanics 38 (1), 87-110.

Naghdi, P.M., 1956. A survey of recent progress in the theory of elastic shells. Applied Mechanics Reviews 9 (9), 365-368.

Noor, A.K., 1973a. Free vibrations of multilayered composite plates. AIAA Journal 11 (7), 1038-1039.

Noor, A.K., 1973b. Mixed finite-difference scheme for analysis of simply supported thick plates. Computers and Structures 3, 967-982.

Noor, A.K., Burton, W.S., 1989. Assessment of shear deformation theories for multilayered composite plates. Applied Mechanics Reviews 42 (1), 1-13.

Pagano, N.J., 1969. Exact solutions for composite laminates in cylindrical bending. Journal of Composite Materials 3, 398-411.

Pagano, N.J., Hatfield, S.J., 1972. Elastic behavior of multilayered bidirectional composites. AIAA Journal 10 (7), 931-933.

Pagano, N.J., exact solutions for rectangular bidirectional composites and sandwich plates. Journal of Composite Materials 4, 20-34.

Paley, M., and Aboudi, J., 1992. Micromechanical analysis of composites by the generalized cells method. Mechanics of Materials 14 (2), 127-139.

Panda, S., Natarajan, R., 1981. Analysis of laminated composite shell structures by finite-element method. Computers & Structures 14 (3-4), 225-230.

Pao, Y. -H., 1989. Adaptive Pattern Recognition and Neural Networks. Addison-Wesley Publishing Company, Reading, Mass.

Rao, K.M., 1990. Analysis of Thick laminated anisotropic composite plates by the finite element method. Composite Structures 15 (3), 185-213.

Rao, K.P., 1978. Rectangular laminated anisotropic shallow thin shell finite-element. Computer Methods in Applied Mechanics and Engineering 15 (1), 13-33.

Reddy, J.N., Chandrashekhara, K., 1985. Geometrically non-linear transient analysis of laminated, doubly curved shells. International Journal of Non-Linear Mechanics 20 (2), 79 - 90.

Reddy, J.N., 1982. Bending of laminated anisotropic shells by a shear deformable finite-element. Fibre Science & Technology 17 (1), 9-24.

Reddy, J.N., 1982. On the solutions to forced motions of rectangular composite plates. Journal of Applied Mechanics 49 (2), 403-408.

Reddy, J.N., 1983. Dynamic (transient) analysis of layered anisotropic composite material plates. International Journal for Numerical Mechods in Engineering 19 (2), 237-55.

Reddy, J.N., 1984. A simple higher-order theory for laminated composite plates. Journal of Applied Mechanics 51 (4), 745-752.

Reddy, J.N., 1984. Energy and Variational Methods in Applied Mechanics. John Wiley and Sons, New York

Reddy, J.N., 1985. A higher-order shear deformation theory of laminated elastic shells. International Journal of Engineering Science 23 (3), 319-330.

Reddy, J.N., 1990. A review of refined theories of composite laminates. Shock and Vibration Digest 22 (7), 3-17.

Reddy, J.N., 1997. Mechanics of Laminated Composite Plates: Theory and Analysis. CRC Press, Inc. Boca Raton, Florida.

Reissner, E. and Stavsky, Y., 1961. Bending and stretching of certain types of aeolotropic elastic plates. Journal of Applied Mechanics, 28, 402—408.

Reissner, E., 1972. A consistent treatment of transverse shear deformations in laminated anisotropic plates. AIAA Journal 10 (5), 716-718.

Reissner, E., 1979. Note on the effect of transverse shear deformation in laminated anisotropic plates. Computer Methods in Applied Mechanics and Engineering 20 (2), 203-209.

Ren, J.G., 1987. Exact solutions for laminated cylindrical shells in cylindrical bending, Composite Science and Technology, 29 (3), 169-187.

Reuss, A., 1929. Berechnung der fliessgrenze von mischkristallen auf grund der plastizitätsbedingung für einkristalle. Z. Angew. Math. Mech. 9, 49-58.

Robbins, D.H., Reddy, J.N., Rostam-Abadi, F., 2004. Towards Hierarchical Modeling of Damage in Composite Structures. 45th AIAA/ASME/ASCE/AHS/ASC Structures, Structural Dynamics & Materials Conference, AIAA, Palm Springs, CA.

Rumelhart, D.E., Hinton, G.E., Williams, R.J., 1986. Learning Internal Representations By Error Propagation. Parallel Distributed Processing: Explorations in the Microstructures of Cognition. Vol. I: Foundations, Eds. D. E. Rumelhart and J. L. McCelland, MIT Press, Cambridge, Mass.

Savoia, M., Reddy, J.N., 1992. A variational approach to three-dimensional elasticity solutions of laminated composite plates. Journal of Applied Mechanics 59, S166-S175.

Shivakumar, K.N., Murty, A.V.K., 1978. High precision ring element for vibrations of laminated shells. Journal of Sound and Vibration 58 (3), 311-318.

Skrzypek, J., Ganczarski, A., 1999. Modeling of Material Damage and Failure of Structures, Springer, Berlin.

Soden, P.D., Hinton, M.J., Kaddour, A.S., 2002. Biaxial test results for strength and deformation of a range of E-glass and carbon fibre reinforced composite laminates:

failure exercise benchmark data. Composites Science and Technology 62 (12-13), 1489-1514.

Soden, P.D., Hinton, M.J., Kaddour, A.S., 1998. A comparison of the predictive capabilities of current failure theories for composite laminates. Composites Science and Technology 58 (7), 1225-1254.

Soden, P.D., Hinton, M.J., Kaddour, A.S., 2002. Biaxial test results for strength and deformation of a range of E-glass and carbon fibre reinforced composite laminates: failure exercise benchmark data. Composites Science and Technology 62 (12-13), 1489-1514.

Specht, D. F., 1990. Probabilistic neural networks. Neural Networks 3, 109-118.

Srinivas, S., Rao, A.K., 1970. Bending, vibration and buckling of simply supported thick orthotropic rectangular plates and laminates. International Journal of Solids and Structures 6, 1463-1481.

Srinivas, S., Rao, C.V.J., Rao, A.K., 1970. An exact analysis for vibration of simply-supported homogeneous and laminated thick rectangular plates. Journal of Sound and Vibration 12 (2), 187-199.

Stavsky, Y., 1961. Bending and stretching of laminated aeolotropic plates. Journal of Engineering Mechanics, ASCE 87 (EM6), 31-56.

Stouffer, D.C., Dame, L.T., 1996. Inelastic Deformation of Metals. Models, Mechanical Properties and Metallurgy. John Wiley and Sons, Inc., New York.

Sun, C.T. and Chen, J.L., 1991. A micromechanics model for plastic behavior of fibrous composites. Composites Science and Technology 40 (2), 115-129.

Sun, C.T., Vaidya, R. S., 1996. Prediction of composite properties from a representative volume element. Composites Science and Technology 56 (2), 171-179.

Sun, H., Di, S., Zhang, N., Wu, C., 2001. Micromechanics of composite materials using multivariable finite element method and homogenization theory. International Journal of Solids and structures 38 (17), 3007-3020.

Swaddiwudhipong S., Liu Z.S., 1997. Response of laminated composite plates and shells. Composite Structures 37 (1), 21-32.

Swift, R.A., Batill, S.M., 1991. Application of Neural Networks to Preliminary Structural Design. AIAA/ASME/ASCE/AHS/ASC 31st Structures, Structural Dynamics and Materials Conference, AIAA-91-1038.

Szewczyk, P.Z., Hajela, P., 1994. Damage detection in structures based on feature-sensitive neural networks. Journal of Computing in Civil Engineering 8(2), 163-178.

Trampczynski, W.A., Hayhurst, D.R., Leckie, F.A., 1981. Creep rupture of copper and aluminum under non-proportional loading. Journal of the Mechanics and Physics of Solids 29, 353-374.

Tamma, K.K., Avila, A.F., 1999. An integrated micro/macro modeling and computational methodology for high temperature composites. Thermal Stresses 5, Lastran Corporation, Rochester, NY. 143-256.

Tiersten, H.F., 1967. Hamilton's Principle for Linear Piezoelectric Media. IEEE Proceedings 55 (8), 1523-1524.

Toledano, A., Murakami, H., 1987. A composite theory for arbitrary laminate configurations. ASME Journal of Applied Mechanics 54, 181-189.

Tsai, S.W., 1968. Strength theories of filamentary structures. Fundamental aspects of fiber reinforced plastic composites, Wiley Interscience, New York, 3-11.

Tsai, S.W., Wu, E.M., 1971. A general theory of strength for anisotropic materials. Journal of Composite Materials 5, 58-80.

Tsou, P., Shen, M. –H. H., 1994. Structural damage detection and identification using neural networks. AIAA Journal 32(1), 176-183.

Vapnik, V., 1995. The Nature of Statistical Learning Theory. Springer Verlag.

Varadan, T.K., Bhaskar, K., 1991. Bending of laminated orthotropic cylindrical shells - an elasticity approach. Composite Structures 17 (2), 141-156.

Varadan, T.K., Bhaskar, K., 1997. Review of different laminate theories for the analysis of composite. Journal of the Aeronautical Society of India 49, 202-208.

Voigt, W., 1989. Über die beziehung zwischen den beiden elastizitätskonstanten isotroper körper. Wied. Ann. 38, 573-587.

Waibel, A., 1989. Phoneme Recognition Using Time Delay Neural Networks. IEEE Proceedings, ASSP-37, 328-339.

Walker, K.P., Freed, A.D., Jordan, E.H., 1991. Microstress analysis of periodic composite. Composites Engineering 1, 29-40.

Walker, K.P., Jordan, E.H., Freed, A.D., 1990. Equivalence of green's function and the fourier series representation of composites with periodic microstructure. Micromechanics and Inhomogeneity, The Toshira Mura 65th Anniversary Volume, Springer, New York, 535-558.

Wan, E., 1994. Time Series Prediction: Forecasting the Future and Understanding the Past. Addison-Wesley Publishing Company, Boston.

Wang, A.S.D., Rose, J.L., Chou, P.C., 1972. Strongly coupled stress waves in heterogeneous plates. AIAA Journal 10 (8), 1088-1090.

Ward, I.M., 1983. Mechanical Properties of Solid Polymers. John Wiley and Sons, New York.

Watkins, S.E., Sanders, G.W., Akhavan, F., Chandrashekhara, K., 2002. modal analysis using fiber optic sensors and neural networks for prediction of composite beam delamination. Smart Materials and Structures 11, 489-495.

Whitney, J.M., Leissa, A.W., 1969. Analysis of heterogeneous anisotropic plates. Journal of Applied Mechanics 36 (2), 261-266.

Whitney, J.M., Pagano, N.J., 1972. Shear deformation in heterogeneous anisotropic plates. Journal of Applied Mechanics 37 (4), 1031-1036.

Whitney, J.M., 1969. The effect of transverse shear deformation in the bending of laminated plates. Journal of Composite Materials 3, 534-547.

Whitney, J.M., 1973. Shear correction factors for orthotropic laminates under static load. Journal of Applied Mechanics 40 (1), 302-304.

Whitney, J.M., 1993. A Laminate Analogy for Micromechanics. Proceedings of The American Society for Composites Eighth Technical Conference, Technomic Publishing Co., Lancaster, PA, 785-794.

Wittrick, W.H., 1987. Analytical three-dimensional elasticity solutions to some plate problems and some observations on Mindlin's plate theory. International Journal of Solids and Structures 23 (4), 441-464.

Wu, X., Ghaboussi, J., Garrett, Jr, J.H., 1992. Use of neural networks in detection of structural damage. Computers and Structures 42(4), 649-659.

Xavier, P.B., Lee, K.H., Chew, C.H., 1993. An improved zigzag model for the bending of laminated composite shells. Composite Structures 26 (3-4), 123-138.

Xia, Z.H., Hu, Y.F., Ellyin, F., 2003. Deformation behavior of an epoxy resin subject to multiaxial loadings. Part II: Constitutive modeling and predictions. Polymer Engineering and Science 43(3).

Yang, P.C., Norris, C.H., Stavsky, Y., 1966. Elastic wave propagation in heterogeneous plates. International Journal of Solids and Structures 2 (4), 665-684.

Zhu, L., Kim, H.S., Chattopadhyay, A., Goldberg, R.K., 2005. Improved transverse shear calculations for rate-dependent analyses of polymer matrix composites. AIAA Journal 43(4), 895-905.

Zienkiewicz, O.C., Taylor, R.L., 2000. The Finite Element Method. Butterworth-Heinemann, Oxford.

Zinoviev, P.A., Lebedeva, O.V., Tairova, L.P., 2002. Coupled analysis of experimental and theoretical results on the deformation and failure of laminated composites under a plane state of stress. Composites Science and Technology 62 (12-13), 1711-1723.

Zinoviev, P.A., Tarakanov, A.I., 1978. On the non-linear deformation of laminated composite materials. Primenenie Plastmass v Mashinostroenii. Trudy MVTU, N16, 72-80 (in Russian)